polymer review

The effect of hydrogen bonding on the phase behaviour of ternary polymer blends

Hongxi Zhang, Dorab E. Bhagwagar, John F. Graf*, Paul C. Painter and Michael M. Coleman†

Department of Materials Science and Engineering, The Pennsylvania State University, University Park, PA 16802, USA

** General Electric Corporation, Parkersburg, WV 26181, USA*

(Received 8 April 1994)

In this paper theoretical and experimental studies of the phase behaviour of ternary polymer blends are reviewed. Particular emphasis is placed upon the effect of specific interactions (hydrogen bonds). The association model developed to predict the phase behaviour of binary hydrogen-bonded polymer blends has been extended to ternary polymer blends. Simulations have been performed to illustrate the major effects of 'physical' (primarily dispersion) and 'chemical' (hydrogen bonding) forces on phase behaviour. Theoretically predicted phase diagrams have also been compared to experimental results obtained from five hydrogen-bonded ternary polymer blend systems. Overall, the agreement is satisfactory. One general conclusion is that it will be very difficult to find ternary polymer blends that exist in a single phase over a wide composition range. Furthermore, in most cases an immiscible binary blend cannot be made homogeneous by introducing a small amount of a third polymer ('compatibilizer').

(Keywords: blends; ternary systems; hydrogen bonds)

INTRODUCTION

One inevitable conclusion of the Flory–Huggins theory is that the vast majority of non-polar high molar mass polymers will not mix. This is a direct consequence of the negligibly small combinatorial entropy of mixing these materials coupled with an unfavourable positive enthalpy of mixing. The probability of finding miscible binary polymer mixtures is enhanced, however, if there are favourable specific interactions present between the dissimilar polymers, such as dipole–dipole interactions, hydrogen bonds and the like[1]. During the past several years we have developed an association model that describes the free energy changes that occur in binary hydrogen-bonded polymer mixtures[1–3]. At the same time comprehensive experimental studies were performed that were designed to assess the predictive capacities of the model[1,4–9]. Overall, the association model has successfully predicted the major trends in hydrogen-bonded binary blends and the agreement between theory and experiment, including those reported from other independent laboratories[10–14], has been remarkably good.

Ternary blends have received much less attention. This is hardly surprising, as the complexity of calculating phase diagrams and problems of experimental accuracy and the interpretation of the results increases dramatically over that of analogous binary blends. Nevertheless, there are good reasons to study the phase behaviour of ternary polymer blend systems. For example, 'Is it possible to increase the range over which ternary blends are miscible by introducing specific interactions?', 'Can we add a polymer (say, PolyB) to an immiscible binary blend (PolyA/PolyC) and render the whole system homogeneous (single phase)?' and 'Will PolyB act as a "compatibilizer" and reduce the overall size of the domains in the heterogeneous ternary blend?' These are commonly asked questions which have important commercial ramifications. As the discovery or design of miscible binary polymer blends has been enhanced by considering systems in which there are strong specific interactions (hydrogen bonds) present, one might reasonably presume that immiscible binary blends might well be 'homogenized' by an appropriate PolyB that can hydrogen bond to both PolyA and PolyC. As we will see, things are not that simple. Ternary polymer blends that are truly homogeneous over wide composition ranges are predicted to be rare indeed.

The thermodynamics of ternary polymer mixtures dates back to the early works on ternary polymer solutions by Scott[15] and Tompa[16], which, in turn, are based on the classic Flory–Huggins lattice model[17,18]. Patterson and co-workers[19,20] and Hsu and Prausnitz[21] extended these concepts and calculated spinodal and binodal phase diagrams, respectively, based on the Scott–Tompa theory for different combinations of binary interaction parameters. The importance of solvent-induced phase separation, the so-called $\Delta\chi$ effect[20,21], was recognized during these studies. Su and Fried[22] further extended the theory to ternary polymer blends and computed spinodals similar to those of Patterson. The so-called repulsion model[23,24] was developed along the same lines to handle blends containing statistical copolymers, to which Cowie[25], Paul[26,27] and their respective co-workers, have compared their experimentally determined ternary phase diagrams. Several other studies involving the comparison of experimental ternary phase diagrams to simulations have

† To whom correspondence should be addressed

0032-3861/94/25/5379–19

also been reported[28-30]. The theoretical basis of all the above studies have their origin in the Flory–Huggins lattice model and carry with them the same limitations. Strong specific interactions and so-called free volume effects are usually ignored. The latter problem has been addressed by Klotz and Cantow[31] who applied Flory's equation of state theory to ternary systems and successfully predicted the general form of the upper critical solution temperature (*UCST*) and lower critical solution temperature (*LCST*) phase behaviour.

Some important guidelines for miscibility in ternary polymer blends have been gained from the above studies. In general, the ternary phase behaviour of polymer blend systems in which there are no strong specific interactions present is primarily governed by the magnitude of the binary interaction parameters, χ_{ij} (or equivalent solubility parameters, δ_i). If just one of the binary interaction parameters is significantly larger than the critical value of χ (i.e. $>\chi_{Crit}$, see later) a large portion of the ternary phase diagram is predicted to be heterogeneous. In addition, there is a driving force towards phase separation if there are significant differences in the interaction parameter values, which produces a $\Delta\chi$ effect.

The effect of strong specific interactions (hydrogen bonds) on the phase behaviour of ternary polymer blends has only recently been addressed in our laboratories[32,33] and independently by a group in Spain[34]. In both cases, the binary association model[1] has been extended to ternary hydrogen bonding polymer mixtures, a topic that we discuss in detail in this paper. An inherent assumption of the association model is that favourable 'chemical' specific interactions can be treated separately from the unfavourable 'physical' ones. Accordingly, the factors affecting the phase behaviour of the ternary blends described above, i.e. the magnitudes of χ_{ij} and $\Delta\chi$, are still operative, but now we must add the further complications of the magnitudes of the equilibrium constants describing self- and inter-association, K_i, and the difference between the effective inter-association equilibrium constants, ΔK. The latter, which we will call the ΔK effect (by analogy to the $\Delta\chi$ effect), reflects the difference in the 'chemical' interaction between the self-associating polymer and the other polymers in the mixture.

Experimentally, the determination of glass transition temperatures (T_gs) by differential scanning calorimetry (d.s.c.) and the observation of the optical clarity have been the primary techniques used to map ternary phase diagrams. To our knowledge, only a very few ternary polymer blends that do not involve strong specific intermolecular interactions (but which are still nonetheless polar) have been reported to be homogeneous over the entire composition range. These include poly(methyl methacrylate) (PMMA)/poly(ethylene oxide) (PEO)/polyepichlorohydrin (PECH)[35], PECH-PMMA-poly(vinyl acetate) (PVAc)[36] and poly(styrene-*co*-maleic anhydride)/poly(styrene-*co*-acrylonitrile)/PMMA [or poly(ethyl methacrylate) (PEMA) or poly(MMA-*co*-acrylonitrile)][37]. A further ternary system that does involve hydrogen bonds, phenoxy/poly(vinyl methyl ether)/poly(ε-caprolactone), has also been reported by Guo[36] to be completely homogeneous. Cloud point temperatures were reported for blend compositions of the ternary blends mentioned above, but many are way above the degradation temperatures of one or more of the components and the results cannot be considered irrefutable. More importantly, conventional second run d.s.c. thermograms were used to determine the number and position of the T_gs. While the obvious presence of more than one T_g is convincing evidence for phase separation, the presence of only one T_g is not sufficient to prove that the particular blend composition is single phase, especially when considering ternary blends[38,39]. Two phases may have different compositions of the three polymers, but at the same time very similar T_gs which may not be resolved in the conventional d.s.c. experiment. Accordingly, while the above ternary systems may indeed be completely miscible, convincing independent evidence from other methods will be required before this conclusion is considered unequivocal.

Published reports of ternary blend systems in which all three binary pairs are miscible, but where there is a region of heterogeneity within the phase diagram (the so-called closed loop phase behaviour) are sparse[25,40,41]. In contrast, the published literature pertaining to ternary polymer mixtures where one binary is immiscible and the other two miscible, is extensive[9,26-30,42-51]. Most of these studies were motivated by the idea that a small amount of a third polymer might act as a compatibilizer and improve the compatibility of binary immiscible polymer blends (in terms of improvement to desired mechanical properties and phase size reduction). Using a small amount of a third polymer to achieve complete ternary miscibility, however, has been of only limited success. The most successful results were reported by Paul and co-workers[26], who found that <0.9% of poly(1,4-cyclohexane dimethylenesuccinate) was sufficient to promote the formation of homogeneous mixtures of the immiscible binary of polycarbonate (PC) and a poly(styrene-*co*-acrylonitrile) copolymer containing 25% acrylonitrile. Far more typical are the results of Landry and co-workers[29]. Polystyrene (PS) is immiscible with PC, but both polymers are miscible with the tetramethyl-substituted polycarbonate (TMPC). However, it required >90% TMPC to produce a single-phase structure, although the addition of TMPC to PS/PC mixtures did reduce the phase size and improve the mechanical properties.

In this work, we focus our attention on the theoretical predictions of the phase behaviour of ternary polymer blend systems that we calculate from our association model. These will be compared to experimental studies of five hydrogen-bonded ternary systems: (1) PVAc/poly(vinyl phenol) (PVPh)/poly(methyl acrylate) (PMA); (2) PVAc/PVPh/poly(styrene-*co*-methyl acrylate) copolymer containing 72 wt% methyl acrylate (denoted STMA[72]); (3) PVAc/PVPh/PEO; (4) PVAc/PVPh/poly(styrene-*co*-2-vinyl pyridine) copolymer containing 70 wt% vinyl pyridine (denoted STVPy[72]); and (5) PMMA/PVPh/PEMA. A sixth system, PMMA/PVPh/poly(tetrahydrofuran) (PTHF) will be briefly considered from a theoretical viewpoint only. D.s.c. is the major tool used in the experimental investigations. In cases where more than one T_g is observed in the thermogram we will conclude that the particular blend composition is heterogeneous. If a single intermediate T_g is observed, the sample will be subjected to a procedure called enthalpy relaxation. This method relies upon the phenomenon of enthalpy recovery in physically aged glassy polymer blends and is sometimes referred to as physical ageing[52-56]. In brief, when a polymer is held at a temperature below

its T_g, a relaxation toward equilibrium occurs, resulting in changes in the physical properties such as density and enthalpy. This enthalpy change can be recovered by heating, which is characterized by an endothermic peak in the heat capacity at the glass transition region. The position and the size of the peak depend on the thermal treatment given and on the structure of the polymer itself. This has formed the basis for a thermal analysis method that can be used to resolve closely occurring T_gs in polymer blends[55–60].

EXPERIMENTAL

The polymers used in this study, together with their molecular weights, T_gs and source, are presented in *Table 1*. All polymers purchased from Polyscience and Aldrich were used as received without further purification. PMA and the styrene-*co*-methyl acrylate copolymer containing 72 wt% methyl acrylate (STMA[72]) have been described previously[61,62]. A styrene-*co*-vinyl pyridine copolymer containing 70 wt% vinyl pyridine (STVPy[70]) was synthesized by free radical solution polymerization at 60°C in toluene using azobisisobutyronitrile (AIBN) as initiator. The copolymer was purified by multiple reprecipitation from dilute benzene solution (5 wt%) into a 10 times excess of petroleum ether. The purified samples were then dried in a vacuum oven at 70°C for 48 h. The molecular weight and copolymer composition were determined by g.p.c. and proton n.m.r. analysis, respectively, in a manner similar to that described before[61,62].

Solutions (2%, wt/vol) of all of the polymers, except PEO, were prepared in THF. In the case of PEO, a 70:30 mixture of THF and chloroform was used to facilitate solution. Blends of various compositions were prepared by mixing appropriate amounts of these solutions. Samples for d.s.c. analysis were made by solution casting onto glass slides under ambient conditions. After the evaporation of the majority of the solvent, samples of ~15 mg were transferred into d.s.c. pans and placed in a vacuum oven at room temperature for a minimum of 24 h and then at 70°C for another 24 h to completely remove any residual solvent. To minimize moisture absorption, the samples were stored in a vacuum desiccator prior to use. Thermal analysis was performed with a Perkin–Elmer differential scanning calorimeter (DSC-7) at a heating rate of 20°C min^{-1}. The sample was initially heated to ≈180°C (above the T_g of the polymer with the highest T_g) and then quenched rapidly to −50°C. The sample was then reheated (second run) and the thermogram recorded. The T_g was taken as the midpoint of the heat capacity change. For those blends that exhibited single T_gs using the conventional second run d.s.c. analysis, enthalpy relaxation experiments were performed. To erase previous thermal history before physical ageing, the sample was heated to a temperature above the T_g for 10 min and then quenched in liquid nitrogen. The samples were then physically aged (annealed) for ~24 h (unless otherwise specified) at a temperature (T_a) of ~20°C below the experimental T_g. The enthalpy relaxation curve is then obtained by immediately performing a d.s.c. scan in the conventional manner.

I.r. spectroscopic measurements were recorded on Digilab model FTS-45 and FTS-60 Fourier transform i.r. (*FT*i.r.) spectrometers at a resolution of 2 cm^{-1}. Spectra recorded at elevated temperature were obtained using a heating cell mounted inside the sample chamber. Temperature was regulated by a Micristar 828D digital process controller, which has a reported accuracy of ±0.1°C. Special attention was paid to ensure that all *FT*i.r. samples were sufficiently thin to be within the absorption range where the Beer–Lambert law is obeyed.

SIMULATIONS

The results of the simulations of the phase behaviour of ternary blends that follow were obtained from a very simple model that we use to describe hydrogen bonding. Nonetheless, the major trends that we wish to emphasize are clearly demonstrated, and it is relatively straightforward to extend the concept to more complex systems.

Let us commence by considering three polymers denoted PolyA, PolyB and PolyC. In common with previous nomenclature, PolyB is capable of self-association through the formation of linear hydrogen-bonded chain-like structures[1]. For the sake of simplicity we will assume that the self-association of PolyB can be adequately represented by one equilibrium constant, K_B (typically employed for polyamides and polyurethanes)[1]:

$$B_h + B_1 \overset{K_B}{\rightleftharpoons} B_{h+1} \qquad (1)$$

PolyA and PolyC do not self-associate, and there are no strong intramolecular interactions (hydrogen bonds) formed between them. Typical examples of these types of polymers include PEO, PMMA, poly(vinyl pyridine), etc. However, PolyA and PolyC have 'acceptor groups' that are able to form hydrogen bonds to PolyB. These hydrogen bonds can be described by the equilibrium

Table 1 Polymers used in this study

Polymer	Symbol	*MW*	T_g (°C)	Source
Poly(4-vinyl phenol)	PVPh	1500–7000	140	Polysciences Inc.
Poly(vinyl acetate)	PVAc	60000	43	Polysciences Inc.
Poly(methyl acrylate)	PMA	21000	22	This laboratory
Styrene-*co*-methyl acrylate (72 wt%)	STMA[72]	10900	45	This laboratory
Poly(ethylene oxide)	PEO	100000	−50	Aldrich Chem. Co.
Poly(methyl methacrylate)	PMMA	64000	105	Aldrich Chem. Co.
Poly(ethyl methacrylate)	PEMA	8400	69	This laboratory
Styrene-*co*-vinyl pyridine (70 wt%)	STVPy[70]	25000	102	This laboratory

constant K_A and K_C, respectively:

$$B_h + A \overset{K_A}{\rightleftharpoons} B_hA \quad (2)$$

$$B_h + C \overset{K_C}{\rightleftharpoons} B_hC \quad (3)$$

The stoichiometric equations relating the equilibrium constants to the volume fractions of the species present and the derivation of an equation describing the free energy of mixing of the hydrogen-bonded blends, $\Delta G_m/RT$, has previously been discussed in detail[1]. Accordingly, we simply present the result for the ternary blend described above:

$$\frac{\Delta G_m}{RT} = \frac{\Phi_A}{r_A N_A}\ln\Phi_A + \frac{\Phi_B}{N_B}\ln\Phi_B + \frac{\Phi_C}{r_C N_C}\ln\Phi_C + \Phi_A\Phi_B\chi_{AB} + \Phi_A\Phi_C\chi_{AC} + \Phi_B\Phi_C\chi_{BC} + \frac{\Delta G_H}{RT} \quad (4)$$

where Φ_B, Φ_A and Φ_C are the volume fractions of PolyB, PolyA and PolyC in the blend, respectively, which have degrees of polymerization, N_i. The parameters $r_A = V_A/V_B$ and $r_C = V_C/V_B$ are the ratios of the segment molar volumes of PolyA to PolyB and PolyC to PolyB, respectively. We emphasize that the polymer/polymer interaction parameters, χ_{ij}, which have permissible values of ≥ 0, are defined in equation (4) by the relationship:

$$\chi_{ij} = \frac{V_B}{RT}(\delta_i - \delta_j)^2 \quad (5)$$

where δ_i and δ_j are the solubility parameters that are calculated from group molar attraction and molar volume constants designed to specifically exclude contributions from hydrogen bonding[1]. Finally, the $\Delta G_H/RT$ term, shown in equation (4), which represents a favourable contribution to the free energy of mixing emanating from the changing pattern of hydrogen bonds in the mixture, is a function of the magnitudes of the various equilibrium constants:

$$\frac{\Delta G_H}{RT} = \Phi_B \ln\left(\frac{\Phi_{B_i}}{\Phi^0_{B_i}}\right) + \frac{\Phi_A}{r_A}\ln\Phi_{A_i} + \frac{\Phi_C}{r_C}\ln\Phi_{C_i} + \Phi_B\left\{[K_B(\Phi_{B_i} - \Phi^0_{B_i})] + \left[(1 - K_B\Phi_{B_i})\left(\frac{\xi+\zeta}{1+\xi+\zeta}\right)\right]\right\} - \left[(1 - K_B\Phi^0_{B_i})\Phi_B\ln\Phi_B + \frac{\Phi_A}{r_A}\ln\Phi_A + \frac{\Phi_C}{r_C}\ln\Phi_C\right] \quad (6)$$

where Φ_{B_i}, Φ_{A_i} and Φ_{C_i} are the corresponding volume fractions of isolated (non-hydrogen-bonded) PolyB, PolyA and PolyC segments, $\xi = K_A\Phi_{A_i}/r_A$ and $\zeta = K_C\Phi_{C_i}/r_C$, and the superscript 0 denotes the pure material. The form of equation (6) is very similar to that obtained for binary blends described in reference 1, except that there are extra terms to account for the additional component of the blend. Equation (6) was originally derived for polymer blends that employ a set of experimentally determined equilibrium constants obtained from appropriate miscible polymer mixtures. The $(1 - K_B\Phi^0_{B_i})$ term in the final term of equation (6) is essentially a semi-empirical excess entropy contribution that corrects for effects associated with chain connectivity[1,63–65].

Conceptually, both the spinodal and binodal phase diagrams of ternary hydrogen-bonded blends can be calculated from the various derivatives of equation (4), but the latter is mathematically difficult and computationally time-consuming. Accordingly, we will restrict ourselves here to the calculation of spinodal phase diagrams, which are relatively easy to calculate and are accurate enough to reveal the general trends in the phase behaviour of ternary polymer blends. The criteria for thermodynamic stability of a ternary polymer mixture at a constant temperature and pressure is expressed by the following relationships:

$$\frac{\Delta G_m}{RT} < 0 \quad (7)$$

$$\begin{vmatrix} \Delta G''_{AA} & \Delta G''_{AB} & \Delta G''_{AC} \\ \Delta G''_{BA} & \Delta G''_{BB} & \Delta G''_{BC} \\ \Delta G''_{CA} & \Delta G''_{CB} & \Delta G''_{CC} \end{vmatrix} > 0 \quad (8)$$

where

$$\Delta G''_{ij} = \frac{\partial^2(\Delta G_m/RT)}{\partial\Phi_i\partial\Phi_j}$$

Equation (8) is equivalent to the following inequalities:

$$\frac{\partial^2(\Delta G_m)}{\partial^2\Phi_A} > 0 \quad (9)$$

and

$$\left[\frac{\partial^2(\Delta G_m)}{\partial^2\Phi_A}\right]\left[\frac{\partial^2(\Delta G_m)}{\partial^2\Phi_B}\right] - \left[\frac{\partial^2(\Delta G_m)}{\partial\Phi_A\partial\Phi_B}\right]^2 > 0 \quad (10)$$

where the derivatives in equations (9) and (10) are calculated with Φ_C as a dependent variable and Φ_A and Φ_B as independent variables.

The computer program written previously to calculate the free energy of mixing, phase diagrams, miscibility windows and maps, etc., of binary hydrogen-bonded blends[1], was modified to permit the calculation of ternary spinodal phase diagrams. To keep things simple, an additional modification to the original program was made so that χ_{ij} values could be introduced directly [equation (4)], as an alternative to the corresponding non-hydrogen bonding solubility parameters [equation (5)]. For the simulations described in this section the following parameters were used, unless otherwise specified. A temperature of 25°C was assumed. Components PolyA, PolyB and PolyC were assumed to have equal degrees of polymerization (i.e. $N_A = N_B = N_C = 500$), with identical segment molar volumes ($V_A = V_B = V_C = 100\ \text{cm}^3\ \text{mol}^{-1}$) and molecular weights, $M_i = 100\ \text{g mol}^{-1}$. Accordingly, in the absence of favourable specific interactions (i.e. $\Delta G_H/RT = 0$), the critical value of χ for each binary blend is $\chi_{Crit} = 0.004$, assuming the validity of the Flory–Huggins equation. In our calculations, all three conditions [i.e. equations (7), (9) and (10)] were tested. Calculated results are displayed in the form of homogeneous (single phase) or heterogeneous (multiphase) regions. For those compositions where the above three conditions are not satisfied, very small open circles are displayed, which indicate that the compositions are heterogeneous. On the other hand, homogeneous compositions are denoted by an unshaded (blank) region. We should emphasize that the true homogeneous region will be overestimated, because we are not accounting for metastable (binodal) regions.

We will commence with the simple case of a ternary

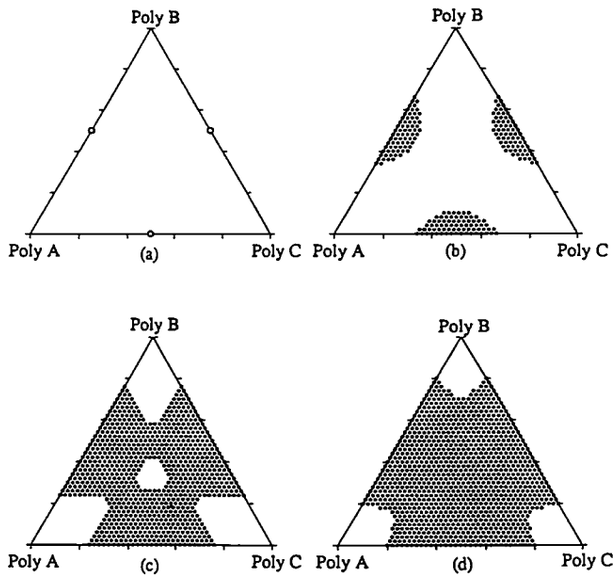

Figure 1 Ternary spinodal phase diagrams illustrating the effect of varying χ values. Calculated from equations (4)–(10) at 25°C. The three polymer repeat units were assumed to have identical molar volumes, $V_i = 100\,cm^3\,mol^{-1}$ and molecular weights, $M_i = 100\,g\,mol^{-1}$. A degree of polymerization, $N_i = 500$, was assumed for all three polymers. Additional restrictions: $\chi_{AB} = \chi_{BC} = \chi_{AC}$ and $K_B = K_A = K_C = 0$. (a) $\chi = 0.004$; (b) $\chi = 0.0045$; (c) $\chi = 0.0055$; (d) $\chi = 0.0065$

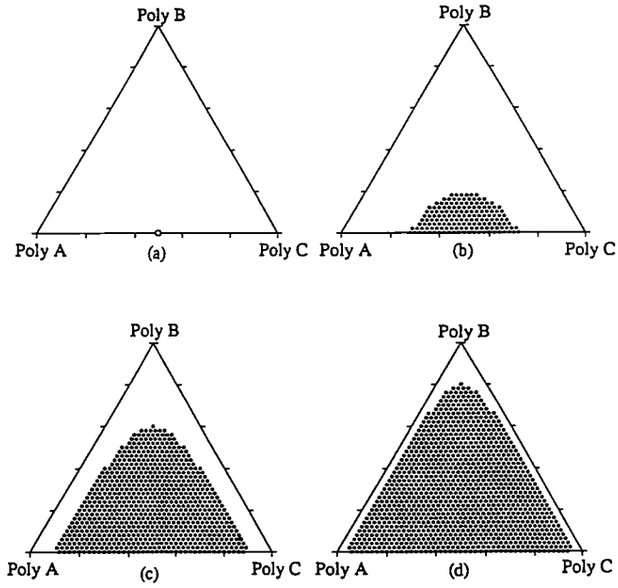

Figure 2 Ternary spinodal phase diagrams illustrating the effect of varying χ values. Calculated at 25°C with constant $V_i = 100\,cm^3\,mol^{-1}$; $M_i = 100\,g\,mol^{-1}$ and $N_i = 500$. Additional restrictions: $\chi_{AB} = \chi_{BC} < 0.004$ and $K_B = K_A = K_C = 0$. (a) $\chi_{AC} = 0.004$; (b) $\chi_{AC} = 0.005$; (c) $\chi_{AC} = 0.01$; (d) $\chi_{AC} = 0.02$

polymer blend system where there are no specific interactions present, so that $K_B = K_A = K_C = 0$. Equation (4) then reduces to the Flory–Huggins equation as $\Delta G_H/RT = 0$ and complete miscibility is predicted when $\chi_{AB} = \chi_{BC} = \chi_{AC} < \chi_{Crit}$. If $\chi_{AB} = \chi_{BC} = \chi_{AC} = \chi_{Crit}$ three critical points are observed at the 50/50 binary compositions (*Figure 1a*). When $\chi_{AB} = \chi_{BC} = \chi_{AC} > \chi_{Crit}$ symmetrically immiscible regions appear along the sides of the triangular plane (*Figure 1b*). These immiscible regions increase and finally merge with one another as the magnitude of χ_{ij} increases, resulting in a phase diagram of three immiscible regions with a central region that is homogeneous (*Figure 1c*). Increasing the magnitude of χ_{ij} further reduces the central region to a point, after which the corresponding three immiscible regions overlap with each other (*Figure 1d*). These results are consistent with those of Su and Fried[22].

Figures 2 and *3* illustrate the effect of changing the relative values of χ_{ij}. If $\chi_{AB} = \chi_{BC} < \chi_{Crit}$, and $\chi_{AC} > \chi_{Crit}$, a heterogeneous area spreading out from the critical point at the midpoint of the PolyA–PolyC axis is observed. This increases with the magnitude of χ_{AC}. At a χ_{AC} value of 0.020, which is not a very large value [corresponding as it does, equation (5), to a solubility parameter difference of only $\approx 0.35\,cal^{1/2}\,cm^{-3/2}$], the vast majority of the ternary polymer phase diagram is heterogeneous. The requirements for miscibility are even more stringent, if we now permit $\chi_{AB} \neq \chi_{BC}$, even though both values are less than χ_{Crit}, as illustrated in *Figure 3*. This is the so-called $\Delta\chi$ effect. The above results agree well with those of Patterson[19,20], Prausnitz[21] and Fried[22] and their respective co-workers. The only difference is the definition of χ. In their studies, χ is permitted to assume negative values in order to take into account contributions from different intermolecular interactions. To reiterate, in our work χ reflects only unfavourable 'physical' forces and only positive values are permitted, with the consequence that certain types of ternary diagrams, such as the so-called closed-loop phase diagram, cannot be observed by simply varying χ. To obtain such diagrams one has to consider the effect of specific intermolecular interactions and this is included in our methodology through the $\Delta G_H/RT$ term of equation (4).

The next question one might ask is, 'What is the effect of self-association on the ternary phase diagram?' For example, 'What happens if PolyB self-associates through hydrogen bonding (e.g. is a polyamide), but hydrogen

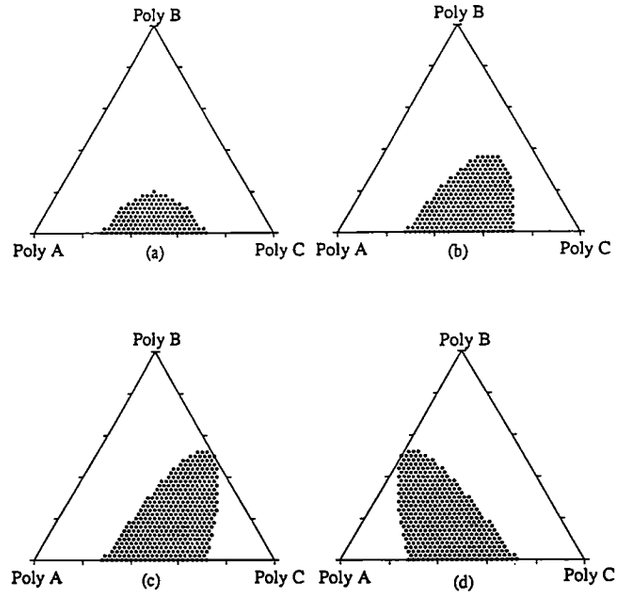

Figure 3 Ternary spinodal phase diagrams illustrating the $\Delta\chi$ effect. Calculated at 25°C with constant $V_i = 100\,cm^3\,mol^{-1}$; $M_i = 100\,g\,mol^{-1}$ and $N_i = 500$. Additional restrictions: $\chi_{AC} = 0.005$ and $K_B = K_A = K_C = 0$. (a) $\chi_{AB} = \chi_{BC} < 0.004$; (b) $\chi_{AB} = 0$, $\chi_{BC} = 0.0035$; (c) $\chi_{AB} = 0$, $\chi_{BC} = 0.004$; (d) $\chi_{AB} = 0.004$, $\chi_{BC} = 0$

bonds cannot form between PolyB and either PolyA or PolyC?' We can simulate this by simply assuming $\chi_{AB}=\chi_{BC}=\chi_{AC}=0$ (equivalent to assuming that the three polymers have identical non-hydrogen bonding solubility parameters) and that $K_A=K_C=0$ (i.e. that inter-association between PolyB and PolyA or PolyC is negligible). This is presented in *Figure 4*. Ternary spinodal phase diagrams are shown that were calculated using values of $K_B=0.02$, 0.2, 2 and 20. Intuitively, one would expect self-association of PolyB to be unfavourable to mixing, which it is, and the heterogeneous area corresponding to a band of PolyB-rich compositions parallel to the PolyA/PolyC axis of the phase diagram increases with increasing magnitude of K_B*.

The next two sets of ternary phase diagrams, shown in *Figures 5* and *6*, illustrate the effect of inter-association. Again, for clarity, we assume $\chi_{AB}=\chi_{BC}=\chi_{AC}=0$ and hold the dimensionless self-association equilibrium constant, K_B, constant at a value of 20. First, let us consider the case where equal values of the inter-association equilibrium constants are employed, i.e. $K_A=K_C$. The effect is quite dramatic. We have seen that when $K_B=20$ and $K_A=K_C=0$ a large symmetric heterogeneous area extending to ~70% PolyB is predicted (*Figure 5a*). Introducing inter-association corresponding to equilibrium constant values of $K_A=K_C=0.2$ reduces the heterogeneous area to ~50% PolyB. Increasing the values further to $K_A=K_C=0.3$ leads to a small heterogeneous band between ~10 and 30% PolyB and for $K_A=K_C\geqslant 0.4$ the entire ternary phase diagram is predicted to be homogeneous. In essence, it is a question of offsetting the unfavourable contribution of self-association to the free energy of mixing with the favourable contributions derived from inter-association†. Balanced inter-association (i.e. $K_A=K_C$) is thus favourable to mixing in ternary hydrogen-bonded blends.

In *Figure 6* we consider the case where $K_A\neq K_C$. Analogous to the $\Delta\chi$ effect, this is a situation that we have chosen to call the ΔK effect and it generally has a negative effect on ternary miscibility. Once again we set $\chi_{AB}=\chi_{BC}=\chi_{AC}=0$ and $K_B=20$ and hold these values constant. Balanced values of $K_A=K_C=20$ were initially employed (which are some 50 times greater in magnitude than those necessary to offset self-association — see *Figure 5*), and a completely homogeneous ternary phase diagram is predicted (*Figure 6a*). If we now calculate the ternary phase diagram with values of K_C twice that of K_A (i.e. $K_A=20$; $K_C=40$), we observe a closed-loop heterogeneous region (*Figure 6b*). Increasing the values of K_C to 100 and 200 leads to much larger areas of heterogeneity (*Figures 6c* and *d*). We should perhaps stress that ΔK values of this magnitude are not atypical (see later) and this demonstrates that even in the case where all three binary mixtures are miscible, large areas of the ternary phase diagram of hydrogen-bonded blends may be heterogeneous simply because of the ΔK effect.

Let us now consider the case where PolyA is not miscible with PolyC, but both PolyA and PolyC are miscible with PolyB. This case has practical ramifications because it addresses the question 'Can I use a hydrogen bonding polymer, say PolyB, to render miscible a mixture of otherwise immiscible polymers PolyA and PolyC?' A simple simulation may be performed by initially setting $\chi_{AB}=\chi_{BC}=0$, $\chi_{AC}=0.005$ and $K_A=K_B=K_C=20$, the result of which is shown in *Figure 7a*. This result is essentially a superposition of

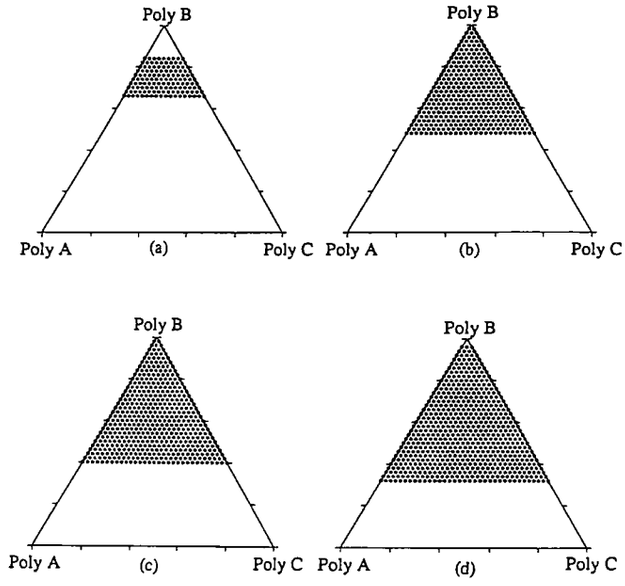

Figure 4 Ternary spinodal phase diagrams illustrating the effect of self-association. Calculated at 25°C with constant $V_i=100\,cm^3\,mol^{-1}$; $M_i=100\,g\,mol^{-1}$ and $N_i=500$. Additional restrictions: $\chi_{AB}=\chi_{BC}=\chi_{AC}=0$ and $K_A=K_C=0$. (a) $K_B=0.02$; (b) $K_B=0.2$; (c) $K_B=2$; (d) $K_B=20$

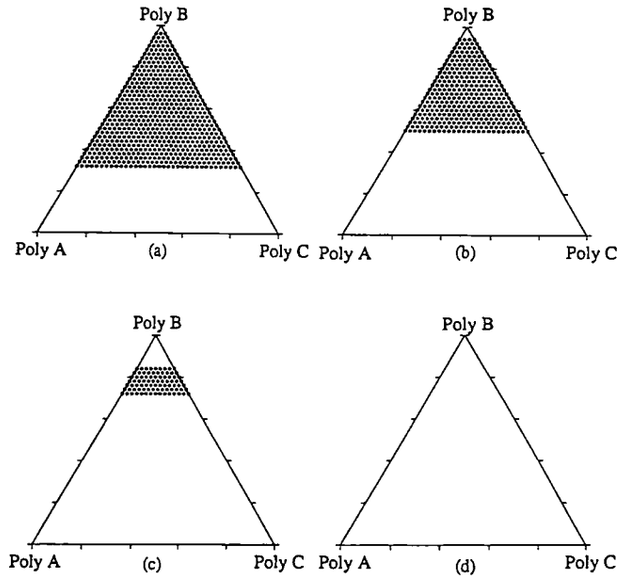

Figure 5 Ternary spinodal phase diagrams illustrating the effect of inter-association. Calculated at 25°C with constant $V_i=100\,cm^3\,mol^{-1}$; $M_i=100\,g\,mol^{-1}$ and $N_i=500$. Additional restrictions: $\chi_{AB}=\chi_{BC}=\chi_{AC}=0$ and $K_B=20$. (a) $K_A=K_C=0$; (b) $K_A=K_C=0.2$; (c) $K_A=K_C=0.3$; (d) $K_A=K_C>0.4$

* Note that the assumed values of K_B only go up to 20, whereas in 'real' polyamides K_B values can be >300 dimensional units

† The reader might question why a homogeneous system is predicted when the values of the inter-association equilibrium constants are less than that of self-association. Equation (4), from which we calculate the free energy of mixing, contains an excess entropy term that accounts for connectivity effects, etc., in hydrogen-bonded polymer blend systems. This permits the use of apparent equilibrium constants obtained experimentally from appropriate miscible polymer blends. The logic of the arguments and the general trends discussed above are not affected, however. Those readers who wish to delve deeper into this subject are referred to references 1, 63, 64 and 65

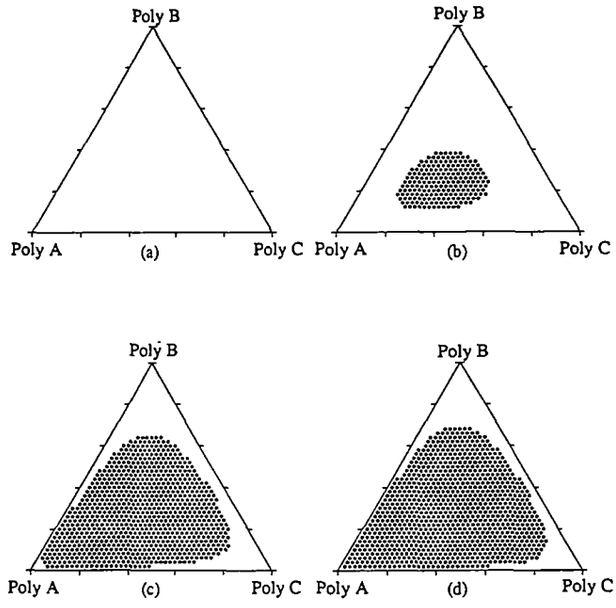

Figure 6 Ternary spinodal phase diagrams illustrating the ΔK effect. Calculated at 25°C with constant $V_i = 100\ cm^3\ mol^{-1}$; $M_i = 100\ g\ mol^{-1}$ and $N_i = 500$. Additional restrictions: $\chi_{AB} = \chi_{BC} = \chi_{AC} = 0$ and $K_B = 20$. (a) $K_A = K_C = 20$; (b) $K_A = 20$, $K_C = 40$; (c) $K_A = 20$, $K_C = 100$; (d) $K_A = 20$, $K_C = 200$

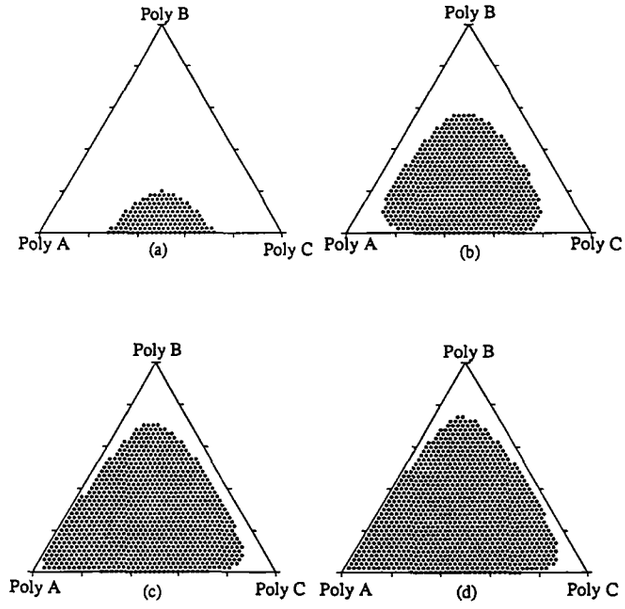

Figure 7 Ternary spinodal phase diagrams illustrating the ΔK effect. Calculated at 25°C with constant $V_i = 100\ cm^3\ mol^{-1}$; $M_i = 100\ g\ mol^{-1}$ and $N_i = 500$. Additional restrictions: $\chi_{AB} = \chi_{BC} = 0$, $\chi_{AC} = 0.005$ and $K_B = 20$. (a) $K_A = K_C = 20$; (b) $K_A = 20$, $K_C = 40$; (c) $K_A = 20$, $K_C = 100$; (d) $K_A = 20$, $K_C = 200$

Figures 2b and *6a*. Note, however, what happens if there is a rather weak ΔK effect, i.e. when $K_A = 20$ and $K_C = 40$ (*Figure 7b*). A much larger heterogeneous area is predicted with increasing ΔK (*Figures 7c* and *d*) and almost fills the spinodal ternary phase diagram at $K_C = 200$. This result does not bode well for those attempting to find hydrogen bonding polymeric homogenizers.

The next simulation addresses the question 'If phase separation in a ternary polymer blend system is predicted on the basis of an unfavourable $\Delta\chi$ effect, is it possible to compensate for this by changing the magnitude of a ΔK effect that works in the opposite sense with respect to composition?' In common with the case considered in the paragraph above, consider a ternary system where PolyA is not miscible with PolyC, but both PolyA and PolyC are miscible with PolyB. However, in this case we introduce a strong $\Delta\chi$ effect by setting $\chi_{AB} = 0.2$, $\chi_{BC} = 0$ and $\chi_{AC} = 0.005$. Initially, $K_A = K_B = K_C = 20$ and the result is shown in *Figure 8a*. A large heterogeneous area covering about two-thirds of the ternary phase diagram is observed. *Figure 8b* shows what happens when the value of K_A is increased to 40. Except for binary PolyA/PolyC compositions from $\approx$25–70% polyA, the entire ternary phase diagram is predicted to be homogeneous. Inter-association of PolyB with PolyA has been accentuated and this serves to counterbalance the rather large positive contribution to the free energy from χ_{AB}. Viewed in another way, we have introduced a ΔK effect by making $K_A > K_C$ which effectively offsets the $\Delta\chi$ effect. Just the opposite trend is predicted if the values of K_A and K_C are reversed (i.e. $K_A = 20$ and $K_C = 40$). Here the $\Delta\chi$ and ΔK effects compound and the vast majority of the ternary phase diagram is heterogeneous (*Figure 8c*). Unfortunately, while the prediction and design of single-phase ternary polymer compositions may appear feasible through the manipulation of the $\Delta\chi$ and ΔK effects, it is likely to be of only limited practical significance (see later).

Further complexity can be introduced by considering ternary blends where two or all of the binary components are immiscible. Such cases are readily simulated, but we will not show these results because the general trends are the same and, unsurprisingly, heterogeneity dominates. We conclude this section by briefly considering the effect of temperature for a couple of specific cases. To reiterate, the values of χ_{ij} solely reflect 'physical' forces and are therefore assumed to have the conventional $1/T$ dependence [equation (5)]. Equilibrium constants are

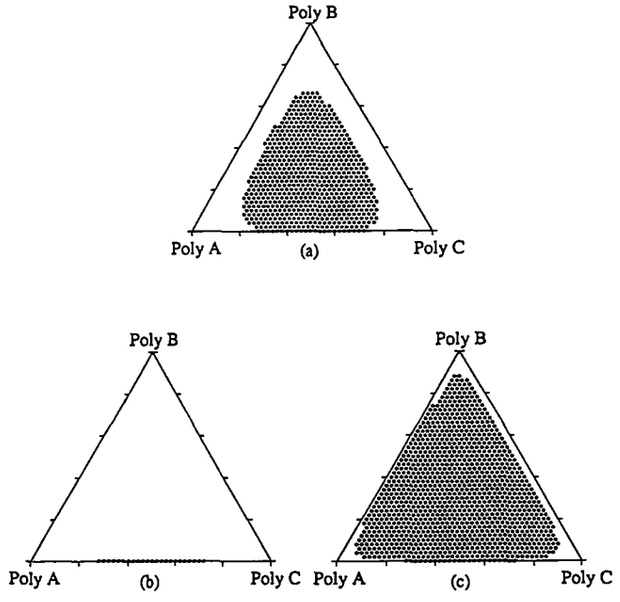

Figure 8 Ternary spinodal phase diagrams illustrating the effect of the combination of the $\Delta\chi$ and ΔK effects. Calculated at 25°C with constant $V_i = 100\ cm^3\ mol^{-1}$; $M_i = 100\ g\ mol^{-1}$ and $N_i = 500$. Additional restrictions: $\chi_{AB} = 0.02$, $\chi_{BC} = 0$, $\chi_{AC} = 0.005$ and $K_B = 20$. (a) $K_A = K_C = 20$; (b) $K_A = 40$, $K_C = 20$; (c) $K_A = 20$, $K_C = 40$

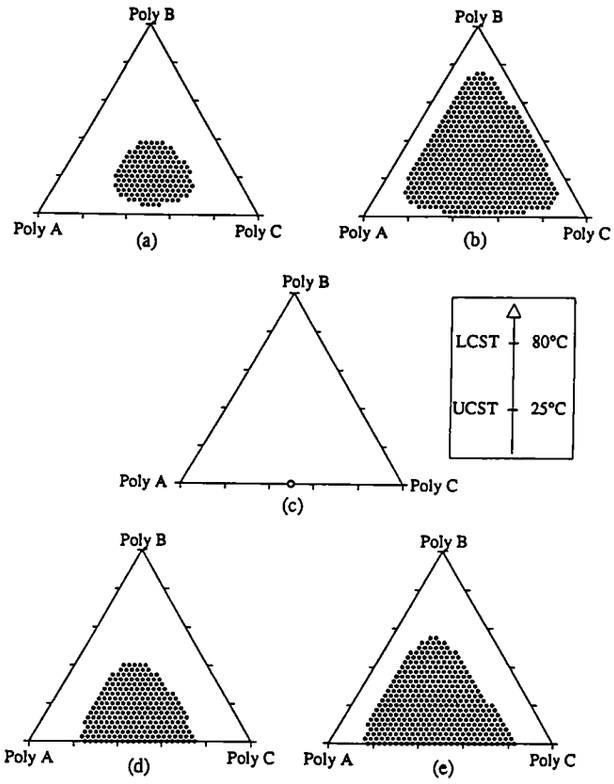

Figure 9 Ternary spinodal phase diagrams calculated as a function of temperature with constant $V_i = 100\ cm^3\ mol^{-1}$; $M_i = 100\ g\ mol^{-1}$ and $N_i = 500$. Additional restrictions: $\chi_{AB} = \chi_{BC} = \chi_{AC} = 0.004$, $K_B = K_A = K_C = 20$ and $h_B = h_C = -5.0$, $h_A = -4.0$ kcal mol^{-1}. (a) 100°C; (b) 200°C; (c) 25°C; (d) −50°C; (e) −100°C

calculated as a function of temperature from the van't Hoff relationship:

$$K_i = K_i^0 \exp\left[-\frac{h_i}{R}\left(\frac{1}{T}-\frac{1}{T^0}\right)\right] \qquad (11)$$

where h_i is the enthalpy of the formation of the hydrogen bond and K_i^0 is the value of the corresponding equilibrium constant at the absolute reference temperature, T^0.

We can use *Figure 1* to illustrate the effect of temperature for a ternary polymer blend system where there are no specific interactions present (i.e. the Flory–Huggins case where $K_B = K_A = K_C = 0$). To reiterate, setting $\chi_{AB} = \chi_{BC} = \chi_{AC} = \chi_{Crit}$ leads to a ternary phase diagram at 25°C (*Figure 1a*) with three critical points, corresponding to the top of the *UCST* at the 50/50 binary compositions. Decreasing the temperature effectively increases the magnitude of χ_{ij} (i.e. $\chi_{AB} = \chi_{BC} = \chi_{AC} > \chi_{Crit}$), and *Figures 1b*, *c* and *d* are equivalent to those calculated at ~ -8, -56 and -90°C, respectively. At temperatures above 25°C, $\chi_{ij} < \chi_{Crit}$, the ternary phase diagram is predicted to be completely homogeneous (remember, there are no free volume effects in the simple Flory–Huggins treatment).

Figure 9 illustrates the effect of temperature on the ternary phase behaviour of a particular system that involves strong specific interactions. Again, to keep things as simple as possible, we set $\chi_{AB} = \chi_{BC} = \chi_{AC} = \chi_{Crit}$. The equilibrium constants describing self- and inter-association $K_B = K_A = K_C$ are given identical values of 20 at 25°C which yields the ternary phase diagram displayed in *Figure 9c*. There is no $\Delta\chi$ effect and the two binaries, PolyB/PolyA and PolyB/PolyC, are miscible. A single critical point is calculated for the other binary PolyA/PolyC at the 50/50 binary composition. For the sake of argument, let us assume values of enthalpies of the hydrogen bonding formation are: $h_B = h_C = -5.0$ and $h_A = -4.0$ kcal mol^{-1}. If we now change the temperature from 25°C to some temperature T_1, we modify the relative contributions to the free energy of mixing [equation (4)] from the χ_{ij} and $\Delta G_H/RT$ terms. The temperature dependence of these two terms, however, is very different. As noted above, the magnitudes of the χ_{ij} terms vary as T^{-1}, and in the particular case considered here, $\chi_{ij} < \chi_{Crit}$ above 25°C. On the other hand, the magnitude of the $\Delta G_H/RT$ term is a function of the various equilibrium constant values, which vary with temperature according to equation (11). Note also that as $h_A \neq h_C$ the values of the equilibrium constants K_A and K_C will not be the same at T_1. Accordingly, this implies a temperature dependent ΔK effect, which in turn affects the form of the predicted ternary phase diagrams. *Figures 9e* and *d* show ternary phase diagrams calculated at temperatures of -100 and -50°C, respectively. A heterogeneous region that spreads out from the PolyA/PolyC axis decreases as the temperature is raised to 25°C, at which temperature the phase diagram is essentially homogeneous. Above 25°C, we observe the appearance of closed-loop heterogeneous regions. This 'reappearance of phases' is very similar to the observations of the *UCST* and *LCST* in binary polymer blends and is considered characteristic of mixtures involving hydrogen bonding components.

In summary, the position, shape and size of the heterogeneous region in ternary phase diagrams of polymer blends that involve strong specific interactions (hydrogen bonds) is a sensitive function of (1) the magnitudes of the individual χ_{ij}, (2) the presence of $\Delta\chi$ effects, (3) the magnitudes of the individual equilibrium constants, K_i, describing self- and inter-association, (4) the presence of ΔK effects caused by differences in the inter-association equilibrium constants, the relative values of the molar volumes of the chemical repeat units, $r_i = V_i/V_B$ (which affects K_A and K_C), and/or the enthalpies of the hydrogen bond formation, h_i and (5) the molecular weight of the individual blend components. We can generally conclude from the simulations that:

1. It will be difficult to find ternary polymer blends that exist in a single phase over a wide composition range. Only in very rare cases, where the 'physical' ($\Delta\chi$) and 'chemical' (ΔK) interaction differences are negligible or finely balanced, can we expect to find miscible ternary polymer blends.
2. In most cases, an immiscible binary blend cannot be made homogeneous by introducing a small amount of a third polymer (compatibilizer).
3. While the presence of specific intermolecular interactions enhances the probability of forming a homogeneous ternary polymer blend, they can concurrently exacerbate the situation through the ΔK effect, which promotes phase separation.

COMPARISON TO EXPERIMENTAL RESULTS

In the simulations discussed above we were deliberately simplistic in our choice of variables in order to illustrate as simply as possible the major trends in the phase behaviour of hydrogen-bonded ternary blends (e.g. all

Table 2 Parameters used in the calculations

Polymer	Molar volume ($cm^3\ mol^{-1}$)	Molecular weight ($g\ mol^{-1}$)	Solubility parameter ($cal^{1/2}\ cm^{-3/2}$)	Association equilibrium constants
PVPh	100	120	10.6	$K_2=21$, $K_B=66.8$
PVAc	70	86	9.6	$K_A=57.5$
PMA	70	86	9.6	$K_C=47.5$
STMA[72]	100	120	9.5	$K_C=47.5$
PEO	38	44	9.4	$K_C=100$ and 200
PMMA	85	100	9.1	$K_C=37.5$
PEMA	101	114	8.9	$K_A=37.5$
STVPy[70]	125	150	10.4	$K_C=598$
PTHF	71	72	8.8	$K_C=88.8$

polymer segments were assumed to have molar volumes of $100\ cm^3\ mol^{-1}$). Now, however, we are going to consider 'real' polymer blend systems for which we can calculate ternary spinodal phase diagrams and compare the predictions with actual experimental observations. Necessary inputs into the computer program that we developed to calculate the free energy of mixing[1] include: (1) the three segment molar volumes, molecular weights and non-hydrogen-bonded solubility parameters; (2) the number-average degree of polymerization of the respective polymers; (3) dimensionless equilibrium constants describing self-association and inter-association that are scaled to the reference volume of the self-association segment*, V_B; and (4) the enthalpies of hydrogen bond formation.

From the simulations described above, it will be challenging indeed to find hydrogen-bonded ternary systems that exist in a single phase over a wide composition range, and even more difficult to find a system that is completely homogeneous. Even in cases where all three binaries are miscible, areas of heterogeneity in the ternary phase diagram are predicted to be the rule, because of the existence of the 'physical' ($\Delta\chi$) and 'chemical' (ΔK) effects. Only in very rare cases, where the $\Delta\chi$ and ΔK interactions are finely balanced, can we expect to find completely miscible ternary polymer blends. Nonetheless, we have found such a system, PVAc/PVPh/PMA, and we will start with a discussion of this blend system. We will then turn our attention to what we originally surmised might be another potentially homogeneous system, PVAc/PVPh/STMA[72], but which in fact turned out to be heterogeneous. Next, we will consider the PVAc/PVPh/PEO system, where all three binaries are miscible, but where there is a large heterogeneous area due in large part to a significant ΔK effect. Then, we will consider the PVAc/PVPh/STVPy[70] and PMMA/PVPh/PEMA systems, where the PVAc/STVPy[70] and PMMA/PEMA binaries are immiscible. Finally, we will consider a system, PMMA/PVPh/PTHF, where we speculate that the ΔK effect might offset the $\Delta\chi$ effect.

* We will have to be careful when we consider the so-called ΔK effect. In the simulations all the molar volumes were fixed at $100\ cm^3\ mol^{-1}$ and ΔK could be directly related to the ratio of K_A to K_C. However, for systems where the molar volumes of the specific repeat units are different, which implies that the number of interacting sites per unit volume varies, ΔK is related to the ratio of 'effective' inter-association equilibrium constants, K'_A/K'_C, where $K'_A=K_A/r_A$ and $K'_C=K_C/r_C$

PVAc/PVPh/PMA ternary blends

Blends of PVAc/PVPh/PMA are the only hydrogen-bonded system that we have found so far that reasonably satisfies the strict theoretical requirements for a completely homogeneous ternary mixture. First, all three binaries are miscible according to previous studies of our own[61,66,67] and those of others[68,69]. Second, the calculated molar volumes and non-hydrogen-bonded solubility parameters of PVAc and PMA determined from group contributions[1] are identical at $69.8\ cm^3\ mol^{-1}$ and $9.6\ cal^{1/2}\ cm^{-3/2}$, respectively, because the 'specific' repeat units of the two polymers are isomorphous (the only difference being the 'direction' of the –COO– group). The value of χ is thus the same for both the PVPh/PVAc and PVPh/PMA binary blends [see equation (5) with $\delta_{PVPh}=10.6\ cal^{1/2}\ cm^{-3/2}$] and this, of course, means there is no $\Delta\chi$ effect. Third, the magnitudes of the dimensionless equilibrium constants describing the inter-association of PVPh with PVAc and PMA are 57.5 and 47.5, respectively[1], and are not very different. Since the enthalpies of hydrogen bond formation for phenolic hydroxyls with acetoxy and acrylate carbonyl groups are very similar (i.e. -4.0 and -3.8 kcal mol^{-1}, respectively), a weak ΔK effect is indicated. Accordingly, one might reasonably expect that the PVPh/PVAc/PMA blend system has a good chance of being completely homogeneous. Indeed, spinodal ternary phase diagrams calculated via equations (4)–(10) using the above parameter values (*Table 2*) are devoid of any heterogeneous areas over the practical temperature range from 0 to 250°C. Thus the theory predicts a homogeneous ternary system. But is this prediction realized experimentally?

Proving whether a ternary polymer blend of a particular composition is a single phase at a given temperature is not a trivial problem. For the studies reported here we have relied heavily on thermal analysis, and particularly the enthalpy relaxation technique[56–60], to determine T_gs. If more than one obvious T_g is observed then one can be confident that the blend is heterogeneous. However, if only one (typically rather broad) T_g exists one cannot be sure that the blend is homogeneous (single phase). It is entirely possible that the system has phase separated into components of compositions that have almost identical T_gs which are simply not resolved. This problem will be particularly acute for blend compositions rich in one of the components (e.g. can we be expected to be able to differentiate between a homogeneous 5:90:5 PolyA/PolyB/PolyC blend and a heterogeneous mixture of two compositions containing say 8:90:2 and 2:90:8

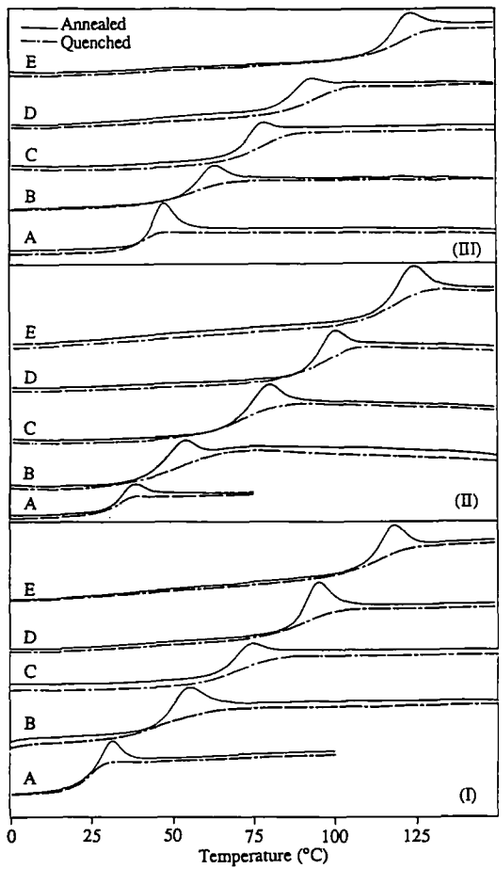

Figure 10 Conventional second run d.s.c. thermograms (dashed lines) and the corresponding thermograms obtained after enthalpy relaxation (solid lines) for ternary PVAc/PVPh/PMA blend compositions. I, II and III correspond to blend compositions in which the binary ratio of PVAc:PMA is 75:25, 50:50, and 25:75, respectively. The labels A–E represent the blend compositions containing 0, 20, 40, 60 and 80 wt% PVPh, respectively

PolyA/PolyB/PolyC, if the T_gs of PolyA are PolyC are not very far apart ?). Hence, if only a single intermediate T_g is observed after careful enthalpy relaxation studies (the resolution of which is reported to be $\approx 2°C$[60]), one can only truly conclude that there is no evidence for phase separation at the resolution and probe size of the experimental method employed.

Figure 10 shows conventional second run d.s.c. thermograms (dashed lines) and the corresponding thermograms obtained after enthalpy relaxation (solid lines) for ternary PVAc/PVPh/PMA blend compositions. The figure is compartmentalized into three major sections denoted I, II and III, which correspond to blend compositions in which the binary ratio of PVAc:PMA is 75:25, 50:50, and 25:75, respectively. The labels A–E represent the blend compositions containing 0, 20, 40, 60 and 80 wt% PVPh, respectively. Thus, for example, the thermograms labelled C in section II were obtained from a blend containing 40% PVPh, 30% PVAc and 30% PMA. A single T_g is observed for all the ternary compositions using conventional second run d.s.c. scans. In addition, all the physically aged samples exhibited a single endothermic peak in the glass transition range, a behaviour consistent with a homogeneous system. A graphical summary of the T_g data is shown in *Figure 11*, which closely approximates the predictions of the Fox equation[70].

In summary, we have no evidence to suggest that any PVAc/PVPh/PMA blend compositions are phase separated at temperatures in the range of 0–150°C. Thus we conclude, until evidence is presented to the contrary, that PVAc/PVPh/PMA blends are completely homogeneous throughout the entire ternary composition range. The experimental results are presented in the bottom diagram of *Figure 12*, where the open circles

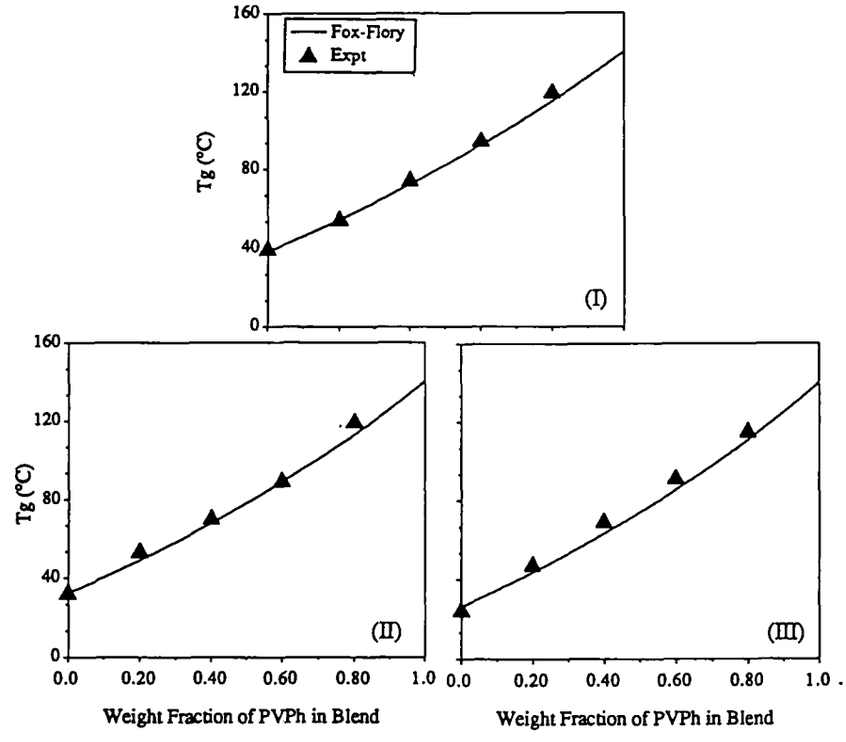

Figure 11 Summary of the T_g data obtained from ternary PVAc/PVPh/PMA blend compositions with binary ratios of (I) 75:25, (II) 50:50 and (III) 25:75 PVAc:PMA

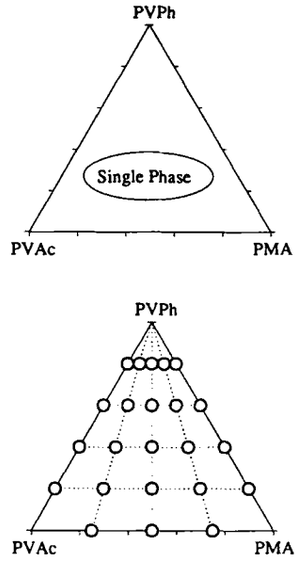

Figure 12 (Top) Theoretical ternary phase diagram for PVAc/PVPh/PMA blends calculated at 25°C using the appropriate parameters listed in *Table 2*. (Bottom) Ternary phase diagram displaying experimental data; the open circles represent compositions exhibiting a single T_g after enthalpy relaxation

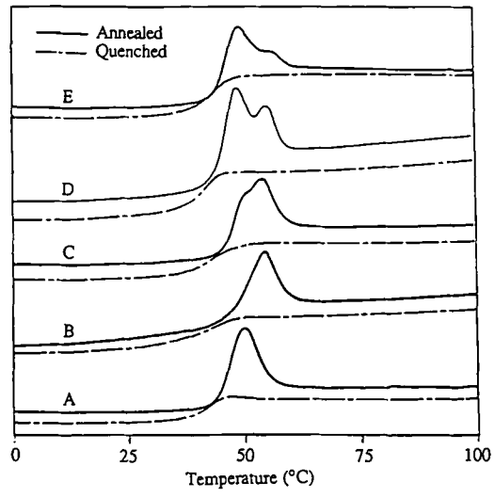

Figure 13 Conventional second run d.s.c. thermograms (dashed lines) and the corresponding thermograms obtained after enthalpy relaxation (solid lines) for (A) pure PVAc, (B) pure STMA[72] and binary PVAc/STMA[72] blends containing (C) 25, (D) 50 and (E) 75 wt% PVAc

represent compositions that exhibited single T_gs and are deemed single phase. For comparison, at the top of *Figure 12* we show the theoretical ternary phase diagram calculated at 25°C. Theory and experiment agree very well in this case.

PVAc/PVPh/STMA[72] ternary blends

We have previously reported on studies of the phase behaviour of binary blends of PVPh and styrene-*co*-methyl acrylate (STMA) copolymers[62]. In essence, PVPh was shown experimentally to be miscible at 150°C with STMA copolymers containing >38 wt% MA and this was found to agree well with the predictions of the association model we developed. STMA[72], the copolymer containing 72 wt% MA, was not chosen arbitrarily for these studies. The calculated non-hydrogen-bonded solubility parameters of the specific repeat units for PS and poly(methyl acrylate) are quite similar[1], 9.5 and 9.6 $cal^{1/2}\,cm^{-3/2}$, respectively, which means that solubility parameter values of random STMA copolymers of any composition are correspondingly similar (in the restricted range of 9.5–9.6 $cal^{1/2}\,cm^{-3/2}$, but we should caution we have not considered errors as yet[1]). This, in turn, implies that the contribution to the free energy of mixing from 'physical' forces (the $\Phi_A\Phi_B\chi$ term) in PVPh/STMA blends is essentially constant regardless of the copolymer composition, which effectively isolates the $\Delta G_H/RT$ term. Hence, the effect of 'dilution', or more precisely, reducing the number of specific interacting sites (carbonyl groups) per unit volume, was studied using STMA copolymers of different styrene concentration[62].

Returning to ternary systems, it occurred to us that as PVPh is miscible with both PVAc and STMA[72] and there is a good chance that PVAc is miscible with STMA[72], because the calculated non-hydrogen-bonded solubility parameters are very close (9.6 and 9.5 $cal^{1/2}\,cm^{-3/2}$, respectively)*, we might have a ternary system in which all the binary blends are miscible. Furthermore, there should be an insignificant $\Delta\chi$ effect, but there exists a definite ΔK effect (the effective K'_A for PVAc is given by $K_A/r_A = 81.7$ as $V_A = 69.8$ and $V_B = 100\,cm^3\,mol^{-1}$, while that of STMA[72], $K'_C = K_C/r_C = 47.5$, as $V_C = 100\,cm^3\,mol^{-1}$). However, PVAc is not miscible with STMA[72] as the enthalpy relaxation studies described below manifestly establish.

Figure 13 shows conventional second run d.s.c. thermograms (dashed lines) and the corresponding thermograms obtained after enthalpy relaxation (solid line) for pure PVAc (denoted A), pure STMA[72] (B) and binary PVAc/STMA[72] blends containing 25, 50 and 75 wt% PVAc (C, D and E, respectively). Note that the T_gs for PVAc and STMA[72] are very close. Single T_gs are observed for all the blend samples using conventional second run d.s.c. scans and, in the absence of further experimentation, one might conclude that the system is miscible (especially when it fits one's preconceived notion!). Following enthalpy relaxation, however, two distinct peaks are observed in the thermograms. This is a beautiful example of the utility of the enthalpy relaxation method and unambiguously proves that the PVAc/STMA[72] blends are immiscible.

The PVAc/PVPh/STMA[72] system thus consists of two miscible binaries, PVPh/PVAc and PVPh/STMA[72], and one immiscible binary, PVAc/STMA[72], that is two phase across a considerable portion of the blend composition range. The question is, 'How large is the heterogeneous area in the ternary phase diagram and does it satisfactorily correspond to that calculated from the association model?' *Figure 14* shows conventional second run d.s.c. thermograms (dashed lines) and three thermograms obtained after enthalpy relaxation (solid lines) for ternary PVAc/PVPh/STMA[72] blend compositions. The figure is again compartmentalized into three major sections denoted I, II and III, which correspond to blend compositions in which the binary ratio of PVAc:STMA[72] is 75:25, 50:50, and

* Note, however, that the number of interacting sites (carbonyl groups) in STMA[72] per unit volume is less than that of PVAc. This 'dilution' lowers the critical value of the solubility parameter difference $(\Delta\delta)_{Crit}$ and is an unfavourable trend for mixing — the reader is referred to reference 1, pages 70–76 for further details

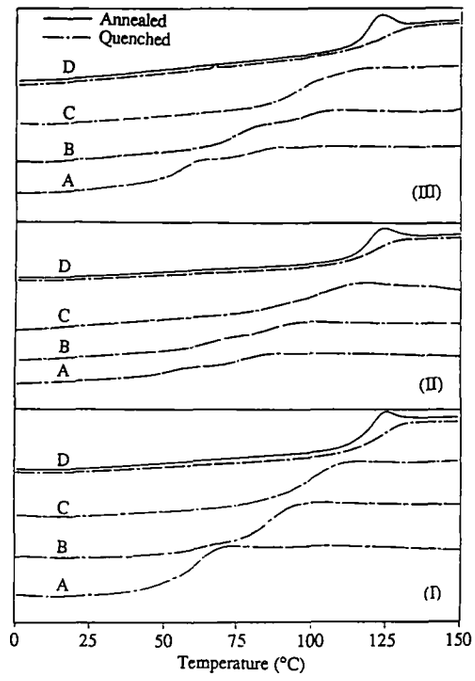

Figure 14 Conventional second run d.s.c. thermograms (dashed lines) and the corresponding thermograms obtained after enthalpy relaxation (solid lines) for ternary PVAc/PVPh/STMA[72] blend compositions. I, II and III correspond to blend compositions in which the binary ratio of PVAc:STMA[72] is 75:25, 50:50, and 25:75, respectively. The labels A–D represent the blend compositions containing 20, 40, 60 and 80 wt% PVPh, respectively

25:75, respectively. The labels A–D represent blend compositions containing 20, 40, 60 and 80 wt% PVPh, respectively. Two T_gs were observed in the conventional second run thermograms for all the ternary compositions, except for blends containing 80 wt% PVPh. Enthalpy relaxation was performed on these latter blends, but there is no evidence of more than one endothermic peak in the glass transition range, a behaviour consistent with a homogeneous system. The experimental results are presented in the bottom diagram of *Figure 15*, with the open and solid circles representing compositions that exhibited one or two T_gs, respectively.

At the top of *Figure 15* we show two different theoretical ternary phase diagrams calculated at 25°C using the parameters listed in *Table 2* and assuming non-hydrogen-bonding solubility parameter values for STMA[72] of 9.5 and 9.4 $cal^{1/2}\,cm^{-3/2}$. If the former value of the STMA[72] solubility parameter is used (the one estimated from group contributions), the binary PVAc/STMA[72] is predicted to be miscible, which is contrary to experimental observations. Note, however, that the majority of the phase diagram (PVPh-rich compositions) is predicted to be heterogeneous, a principal consequence of the ΔK effect mentioned above. Reducing the value of the STMA[72] solubility parameter by only 0.1 $cal^{1/2}\,cm^{-3/2}$ to 9.4 $cal^{1/2}\,cm^{-3/2}$, however, which is well within the error limits of the calculation[1] (± 0.4 $cal^{1/2}\,cm^{-3/2}$), predicts an immiscible PVAc/STMA[72] binary that does match experimental observations quite well. The only inconsistency is that the theory predicts phase-separated compositions rich in PVPh, whereas only single T_gs were observed in the blends containing 80% PVPh, implying that we have single-phase materials. (We caution, however, that we cannot be entirely certain of this experimental conclusion, because we are at the limit of the resolution of thermal analysis. This is especially true for blend compositions that are very rich in PolyB and contain minor components of PolyA and PolyC which possess very close T_gs.)

FT*i.r. spectroscopy and its application to ternary blends*

At this point we will digress from the main thrust of this paper to briefly discuss why *FT*i.r. spectroscopy, which was the primary analytical tool that we used previously to quantitatively characterize binary PVPh/PVAc and PVPh/PMA blends[61,66,67], is not very useful for analogous ternary blends such as the PVAc/PVPh/PMA and PVAc/PVPh/STMA[72] systems discussed above. For binary blends, assuming we know the values of the equilibrium constants describing self- and inter-association and the corresponding enthalpies of hydrogen bond formation, we can readily calculate from the stoichiometric equations the fraction of 'free' (non-hydrogen-bonded) carbonyls, $f_F^{C=O}$, that will be present in a single phase of a blend of any composition and temperature[1]. If the experimental $f_F^{C=O}$ value obtained from *FT*i.r. spectroscopy matches (within error) the theoretical value we can confidently conclude that the material is a single phase. On the other hand, if the experimental $f_F^{C=O}$ value is significantly greater than that calculated, phase separation must have occurred. Using simple lever rule principles it is possible in certain blends to determine a phase diagram from such data[71].

For ternary systems things are not so simple. In blends such as PVAc/PVPh/PMA we first have to recognize that we are dealing with two carbonyl groups, and the carbonyl stretching frequencies of the PVAc acetoxy and the PMA (or STMA[72]) acrylate specific repeats are not well resolved. Nevertheless, it is still experimentally feasible to determine, with reasonable accuracy, the total

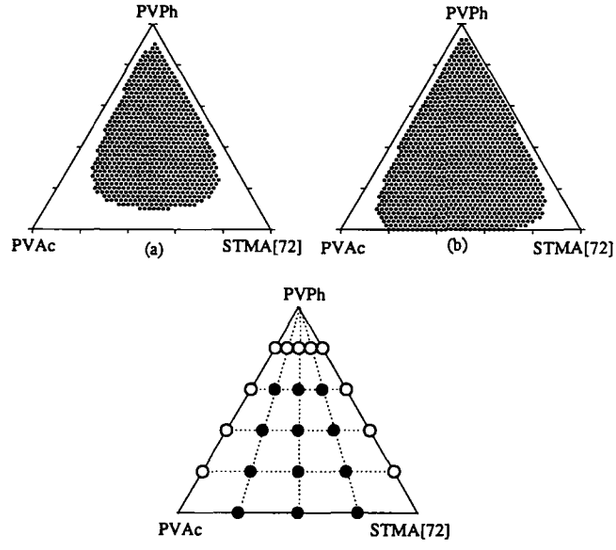

Figure 15 (Top) Theoretical ternary phase diagrams for PVAc/PVPh/STMA[72] blends calculated at 25°C using the appropriate parameters listed in *Table 2* and non-hydrogen-bonded solubility parameter values for STMA[72] of (a) 9.5 and (b) 9.4 $cal^{1/2}\,cm^{-3/2}$. (Bottom) Ternary phase diagram displaying experimental data; the open circles represent compositions exhibiting a single T_g after enthalpy relaxation and the solid circles represent compositions exhibiting two T_gs

fraction of 'free' carbonyl groups for a given ternary blend. Examples of representative i.r. spectra obtained from PVAc/PVPh/PMA blend samples are shown in *Figure 16* and $f_F^{C=O}$ data obtained from such spectra for both the PVAc/PVPh/PMA and PVAc/PVPh/STMA[72] ternary blends are given in *Table 3*. The calculation of the theoretical $f_F^{C=O}$ for homogeneous (single phase) compositions from the stoichiometric equations describing the ternary blends has been discussed before and is quite straightforward[1,32].

Figure 17 shows a comparison of the theoretical homogeneous blend curves of $f_F^{C=O}$ as a function of volume fraction of PVPh to the experimental $f_F^{C=O}$ data for PVAc/PVPh/PMA (denoted A) and PVAc/PVPh/STMA[72] (B) blends. Points corresponding to $f_F^{C=O}$ data obtained from blend compositions that were shown independently (above) to have single intermediate T_gs are indicated by open triangles in *Figure 17*. Conversely, solid triangles represent blend compositions that were shown to have two T_gs. Let us first consider the PVAc/PVPh/PMA blends, which we concluded from thermal analysis are completely homogeneous in equilibrium at ambient temperature. The experimental $f_F^{C=O}$ data points lie, within error, on the theoretical curve for a homogeneous blend and this result appears to confirm the thermal analysis results. We say 'appears' because we would be forced to the same conclusion for the PVAc/PVPh/STMA[72] blends (*Figure 17B*) if the only

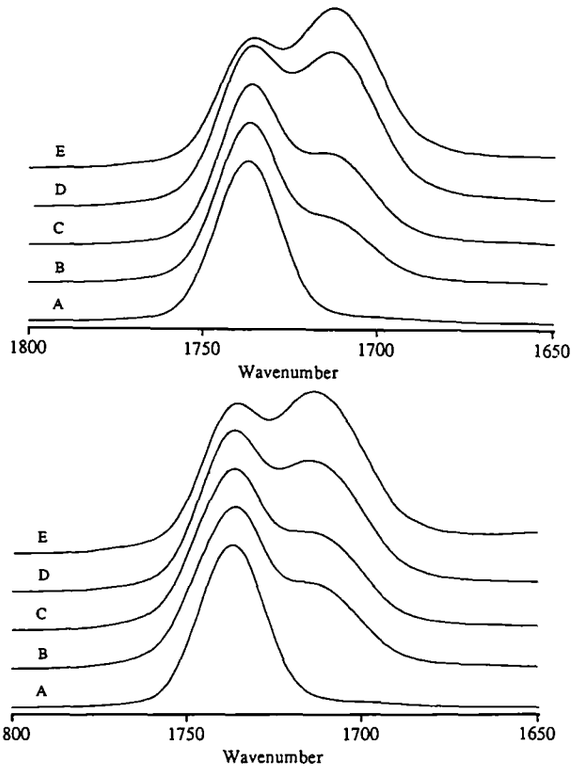

Figure 16 I.r. spectra in the carbonyl stretching region recorded at 150°C. (Top) PVAc/PVPh/STMA[72] and (bottom) PVAc/PVPh/PMA blend compositions containing (A) 50:0:50, (B) 40:20:40, (c) 30:40:30, (D) 20:60:20 and (E) 10:80:10

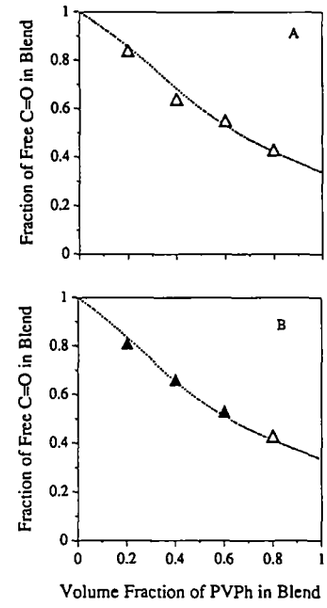

Figure 17 Calculated theoretical fraction of free carbonyl groups (dotted lines) at 150°C as a function of volume fraction VPh for (A) PVAc/PVPh/PMA and (B) PVAc/PVPh/STMA[72] blends. Experimental single intermediate T_gs are indicated by open triangles while those blends exhibiting two T_gs are indicated by solid triangles

Table 3 Curve resolving data of PVAc:PVPh:STMA blends at 150°C

Blend composition (wt%)	'Free' C=O band			H-bonded C=O band			Fraction of free C=O	
	n (cm^{-1})	$W_{1/2}$ (cm^{-1})	Area	n (cm^{-1})	$W_{1/2}$ (cm^{-1})	Area	Expt	Theory[a]
PVAc:PVPh:PMA								
40:20:40	1738	21	9.94	1716	28	2.84	0.84	0.85
30:40:30	1739	20	13.2	1717	28	11.3	0.64	0.67
20:60:20	1739	21	13.2	1716	28	16.2	0.55	0.51
10:80:10	1739	19	12.3	1717	30	24.8	0.43	0.39
PVAc:PVPh:STMA[72]								
40:20:40	1739	21[b]	6.20	1716	27[b]	2.18	0.81	0.83
30:40:30	1738	21[b]	6.95	1716	27[b]	5.32	0.66	0.64
20:60:20	1738	20	3.81	1716	28	5.00	0.53	0.48
10:80:10	1739	20	3.73	1716	30	7.30	0.43	0.38

[a] $K_2=21$, $K_B=66.8$, $K_A=57.5$ and $K_C=47.5$ at 25°C. $h_2=-5.6$, $h_B=-5.2$, $h_A=-3.8$ and $h_C=-4.0$ kcal mol^{-1}
[b] Fixed parameter

criterion was a good match of the experimental $f_F^{C=O}$ data points to the theoretical homogeneous blend curve (three of the ternary blend compositions in question have been shown to exhibit two T_gs, but lie almost perfectly on the theoretical curve). To understand the reason for this apparent anomaly it is best to consider a hypothetical example. Let us say we have a PVAc/PVPh/STMA[72] blend having a composition of 20:60:20 wt%. If the blend exists in a single phase the theoretical $f_F^{C=O}$ is 0.514. If, for the sake of argument, the blend was now to phase separate to the tie lines corresponding to the miscible binary PVPh/PVAc and PVPh/STMA[72] blends drawn parallel to the PVAc/STMA[72] axis (*Figure 15*), from the lever rule we would have half the material with a composition of 40:60:0 and the other half with 0:60:40. Calculating the theoretical $f_F^{C=O}$ for the two miscible binaries is trivial[1] (0.524 and 0.508, respectively) and averaging the two contributions leads to a total $f_F^{C=O}$ equal to 0.517 for the phase-separated blend. This is very close to the value calculated for the homogeneous ternary blend and certainly within the error of measurement. Note also we chose a rather extreme phase separation path and there are numerous other intermediate compositions into which the three components may distribute. The important point is that conformity of the experimentally determined $f_F^{C=O}$ data to the theoretical homogeneous $f_F^{C=O}$ curve is not sufficient to establish a single phase in ternary systems. Conversely, significant deviations of the experimentally determined $f_F^{C=O}$ data to the theoretical homogeneous $f_F^{C=O}$ curve still indicate phase separation, however.

If additional information could be obtained, such as the individual fractions of hydrogen-bonded carbonyls for both PVAc and STMA[72] in ternary blends of varying composition, it might be possible to test whether or not the blend was a single phase. As mentioned above, this is not spectroscopically feasible for the PVAc/PVPh/STMA[72] blends. Pomposo *et al.*[34] did attempt to deconvolute the hydrogen-bonded carbonyl band into two components using spectra obtained from PMMA/PVPh/PEMA blends, but there is no visual evidence that two separate bands exist, and we are not convinced that the results are meaningful (bands must usually be separated by at least half their half-width to be resolved successfully). One combination where it might be possible to independently determine the fraction of hydrogen-bonded carbonyl groups of two of the components in a ternary blend is a system which contains PVPh together with an aliphatic polycarbonate and an aliphatic polyester (or similar polymer with an ester-type functionality). The carbonyl stretching frequencies of the carbonate and ester moieties are well separated from one another and we intend to study such blends in the near future.

PVAc/PVPh/PEO ternary blends

The above discussion on the application of *FT*i.r. spectroscopy to the study of hydrogen-bonded ternary blends is particularly relevant to the PVAc/PVPh/PEO system. PVPh forms single-phase binary mixtures with PVAc and PEO[72-74] in the amorphous state across the entire composition range. The third binary, PEO/PVAc, is also miscible[75-78], a result that we have attributed to their closely matched non-hydrogen-bonded solubility parameters and the presence of weak, but favourable, polar forces[1,32]. Thus, once again, all the three binary blends are miscible in the amorphous state over a significant range of temperature from ambient to the onset of thermal degradation. The question is, 'Are the ternary compositions miscible?' The $\Delta\chi$ effect should be quite small, as the solubility parameters of PVAc and PEO are very close ($\delta_{PVAc} = 9.6$, $\delta_{PEO} = 9.4$ cal$^{1/2}$ cm$^{-3/2}$, respectively). On the other hand, the 'chemical' ΔK effect is likely to be significant, because the equilibrium constant describing the interaction between phenolic hydroxyls and ether oxygens in PVPh/PEO blends is known to be greater than that occurring between phenolic hydroxyls and acetoxy carbonyls in PVPh/PVAc blends. Thus from the simulations discussed above (*Figure 6*), we might anticipate a closed-loop type of phase behaviour, but the question remains, 'How large is the heterogeneous region?'

This question is particularly germane to the interpretation of the i.r. results that we obtained on the PVAc/PVPh/PEO system[32]. In these studies, which were performed before we had written the computer program to calculate the free energy of mixing and spinodals for ternary blends, we made the assumption that homogeneous blends of PVAc/PVPh/PEO were most likely to be found in blend compositions rich in PVPh. Indeed, conventional second run d.s.c. thermograms of blends containing 60% PVPh exhibited single T_gs and appeared to confirm this hypothesis (see Figure 2, ref. 49). The primary objective of these prior studies was to determine the inter-association equilibrium constant, K_C, that describes the interaction of phenolic hydroxyl groups with the ether oxygen of PEO, which cannot be determined directly from the PVPh/PEO binary system. I.r. spectroscopy was used to measure the fraction of hydrogen-bonded PVAc carbonyl groups in PVPh-rich ternary blends of varying compositions. These data were then used to calculate K_C using the concept of competing equilibria and the appropriate stoichiometric equations. At the time we were confident that the blends were single phase, and a dimensionless K_C value was determined which was some five times greater than the analogous K_A value corresponding to the interaction of phenolic hydroxyl groups with acetoxy carbonyls (at 150°C). This result must now be seriously questioned. An accurate determination of K_C can only be obtained from the above methodology if the ternary blends are truly homogeneous. If the blend samples were, in fact, heterogeneous, then the value of K_C would be overestimated to an extent that is a function of the actual composition of the individual phases. As we will see below, enthalpy relaxation studies now reveal that the ternary blends analysed were actually heterogeneous. Furthermore, the theoretical spinodal ternary phase diagram predicts a large heterogeneous closed-loop area in the phase diagram, which extends into the PVPh-rich compositions. This only serves to emphasize how careful one must be in drawing the conclusion that a particular ternary blend is homogeneous (single phase) from experimental thermal or spectroscopic data.

The presence of PEO crystallinity can complicate the interpretation of the d.s.c. thermograms of the blends, but we determined that rapid quenching from 180°C after the first scan effectively eliminated PEO crystallinity in blends where the PVPh content was >30 wt%, as illustrated by the thermograms of PVPh/PEO mixtures in *Figure 18* (curves C–H). *Figure 19* shows conventional second run d.s.c. thermograms (dashed lines) and five

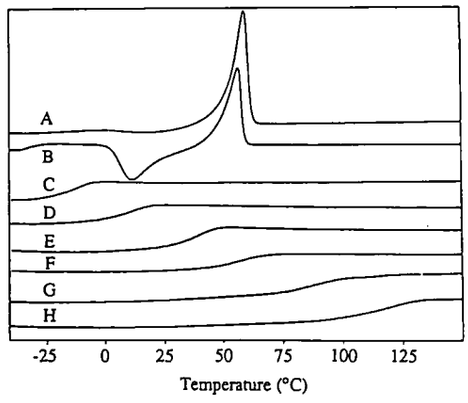

Figure 18 Conventional second run d.s.c. thermograms recorded after rapid quenching from 180°C for binary PVPh/PEO blend compositions containing (A) 20, (B) 30, (C) 40, (D) 50, (E) 60, (F) 70, (G) 80 and (H) 90 wt% PVPh

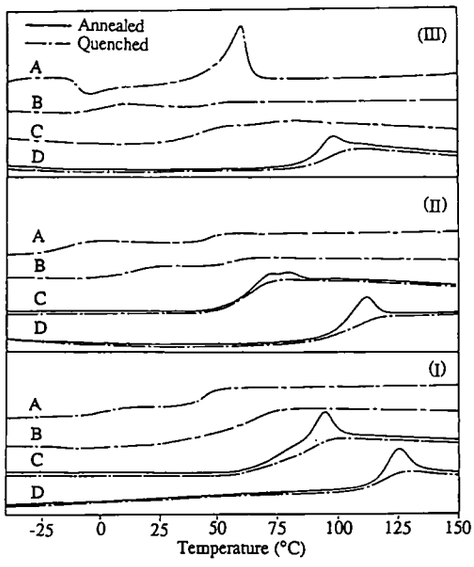

Figure 19 Conventional second run d.s.c. thermograms (dashed lines) and the corresponding thermograms obtained after enthalpy relaxation (solid lines) for ternary PVAc/PVPh/PEO blend compositions. I, II and III correspond to blend compositions in which the binary ratio of PVAc:PEO is 75:25, 50:50, and 25:75, respectively. The labels A–D represent the blend compositions containing 20, 40, 60 and 80 wt% PVPh, respectively

thermograms obtained after enthalpy relaxation (solid lines) for ternary PVAc/PVPh/PEO blend compositions. The three major sections denoted I, II and III, correspond to blend compositions in which the binary ratio of PVAc:PEO is 75:25, 50:50, and 25:75, respectively. The labels A–D represent blend compositions containing 20, 40, 60 and 80 wt% PVPh, respectively. Starting with the blends containing a ratio of PVAc:PEO of 75:25 (section I), we observe two distinct T_gs in the compositions containing 20, 40 and 60 wt% PVPh (the latter confirmed by enthalpy relaxation), which indicates the presence of more than one phase. There is no evidence of more than one endothermic peak in the glass transition range for the blend containing 80% PVPh (thermogram I-D), however, a behaviour consistent with a homogeneous system. A similar trend is observed for the blends containing a 50:50 ratio of PVAc:PEO (section II). Of particular bearing to the discussion presented in the previous paragraph is that the apparent single T_g in the conventional second run d.s.c. scan for the blend containing 60% PVPh (thermogram II-C) is resolved into two components by enthalpy relaxation. Finally, for the blends with a 25:75 ratio of PVAc:PEO (section III), the blends containing 40 and 60% PVPh have two distinct T_gs, while those containing 20 and 80% PVPh we conclude are equivocal. The former is complicated by PEO crystallinity, while the latter appears to exhibit a single T_g by conventional second run d.s.c., but there is a hint of a second endothermic peak following enthalpy relaxation.

The experimental results are summarized in the bottom diagram of *Figure 20*. The open and solid circles again represent compositions that exhibited one or two T_gs, respectively, while equivocal results are designated by the diamond symbol. At the top of *Figure 20* we show two different theoretical ternary phase diagrams calculated at 25°C using the association model with parameter values listed in *Table 2*. As mentioned above, the value of the dimensionless inter-association equilibrium constant that describes the interaction between phenolic hydroxyls and ether oxygens was overestimated in our previous work ($K_C=490$ at 25°C)[49], because we now know the PVAc/PVPh/PEO blends studied were not homogeneous. Accordingly, we still do not have an accurate value of K_C. Nonetheless, ternary spinodal phase diagrams have been calculated with different values of K_C from 100 (close to that determined by Powell and West[79] for low molecular weight analogues) to 500. The trend is obvious and illustrated by the results shown in *Figure 20* for values of $K_C=100$ and 200 at 25°C, respectively. Note that a large portion of the phase diagram emanating from close to the PVPh/PVAc axis is predicted to be heterogeneous, and the size of the closed loop increases with the magnitude

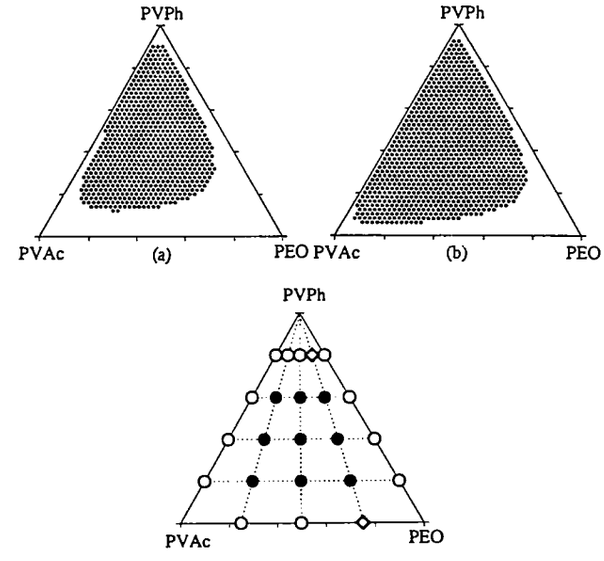

Figure 20 (Top) Theoretical ternary phase diagrams for PVAc/PVPh/PEO blends calculated at 25°C using the appropriate parameters listed in *Table 2* and inter-association equilibrium constant values of (a) $K_C=100$ and (b) $K_C=200$. (Bottom) Ternary phase diagram displaying experimental data; the open circles represent compositions exhibiting a single T_g after enthalpy relaxation, the solid circles represent compositions exhibiting two T_gs and the diamond represents compositions for which the number of T_gs is ambiguous

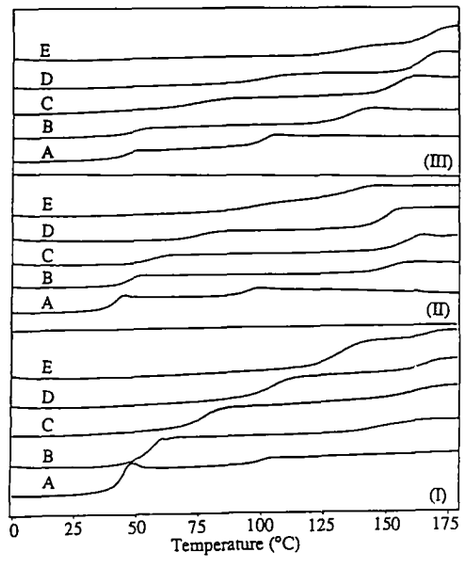

Figure 21 Conventional second run d.s.c. thermograms for ternary PVAc/PVPh/STVPy[70] blend compositions. I, II and III correspond to blend compositions in which the binary ratio of PVAc:STVPy[70] is 75:25, 50:50, and 25:75, respectively. The labels A–E represent the blend compositions containing 0, 20, 40, 60 and 80 wt% PVPh, respectively

of K_C. This is principally a consequence of the ΔK effect. The molar volume of the specific repeat of PEO is rather small (38.1 $cm^3 mol^{-1}$ by group contributions) and this exacerbates the situation. (The effective K'_A for PVAc is 81.7 while that of PEO, $K'_C = 262$, assuming $K_C = 100$.) The upshot of these results is that although the three binaries are miscible, most of the ternary compositions of PVAc/PVPh/PEO blends are heterogeneous. [Remember, we are only calculating spinodals (the heterogeneous area determined from binodals will be greater) and free volume effects have not been taken into account.] This again is not good news for those wishing to employ a hydrogen bonding polymer (PolyB) as a homogenizer for two other immiscible polymers (PolyA and PolyC), a fact that is exemplified by the results obtained on the next ternary system that we will discuss.

PVAc/PVPh/STVPy[70] ternary blends

Limited miscibility studies of binary blends of PVPh and styrene-*co*-2-vinyl pyridine (STVPy) copolymers have been reported by Meftahi and Frechet[80]. These experimental results are in reasonable accord with a predicted miscibility gap extending from pure PVPy to STVPy copolymers containing up to ≈80% ST that was calculated using the association model[1]. PVAc and the STVPy copolymer containing 70 wt% VPy, denoted STVPy[70], are miscible with PVPh. The third binary, PVAc/STVPy[70], is predicted to be immiscible*, which is hardly surprising as the calculated non-hydrogen-bonded solubility parameters of the specific repeat units for PVAc and STVPy[70] are 9.6 and 10.4 $cal^{1/2} cm^{-3/2}$, respectively[1].

Let us pose the following question, one that is commonly encountered in industrial circles. Say I have PolyA which is immiscible with PolyC, 'Can I make a homogeneous system by adding some, hopefully a small amount, of PolyB which is inherently miscible with both PolyA and PolyC?' Unfortunately, the answer is that it is extremely unlikely. Take the PVAc/PVPh/STVPy[70] system, for example. First, there is a significant $\Delta\chi$ effect arising from the different solubility parameters of PVAc and STVPy[70]. Second, there is a large ΔK effect. The dimensionless inter-association equilibrium constant that describes the interaction between the phenolic hydroxyl and pyridine nitrogen K_C is ≈600[1], an order of magnitude greater than that describing the corresponding interaction with acetoxy carbonyls. Differences in the molar volumes of the respective specific repeat units of PVAc and STVPy[70] do not materially affect the argument. Furthermore, the two effects, $\Delta\chi$ and ΔK, do not compensate one another.

Figure 21 shows conventional second run d.s.c. thermograms for ternary PVAc/PVPh/STVPy[70] blend compositions. The three major sections denoted I, II and III, correspond to blend compositions in which the binary ratio of PVAc:STVPy[70] is 75:25, 50:50, and 25:75, respectively. The labels A–E represent blend compositions containing 0, 20, 40, 60 and 80 wt% PVPh, respectively. All of the thermograms exhibit two distinct T_gs, which verifies that they are all heterogeneous. The experimental results are summarized in the bottom diagram of *Figure 22*. The open and solid circles again represent compositions that exhibited one or two T_gs. At the top of *Figure 22* is shown the theoretical ternary phase diagram calculated at 25°C using the association model with parameter values listed in *Table 2*. To all intents and purposes, all ternary blend compositions are predicted to be heterogeneous. Only in extremely PVPh-rich compositions, or compositions very close to the edges of the binary PVPh/PVAc and PVPh/STVPh axes, are the blends predicted to be homogeneous. One must conclude, therefore, that no practical amount of PVPh can be added to a mixture of PVAc and STVPy[70]

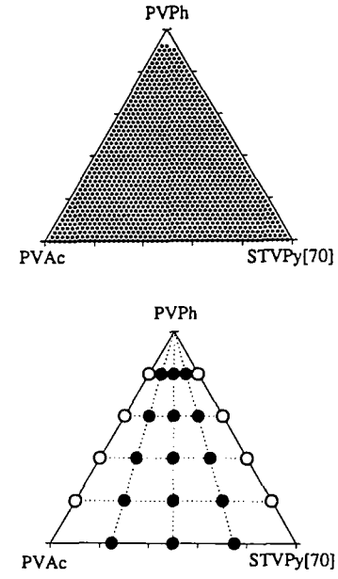

Figure 22 (Top) Theoretical ternary phase diagram for PVAc/PVPh/STVPh[70] blends calculated at 25°C using the appropriate parameters listed in *Table 2*. (Bottom) Ternary phase diagram displaying experimental data; the open circles represent compositions exhibiting a single T_g and the solid circles represent compositions exhibiting two T_gs

* Ref. 1 predicts that PVAc will be immiscible with random STVPy copolymers containing >40 wt% VPy

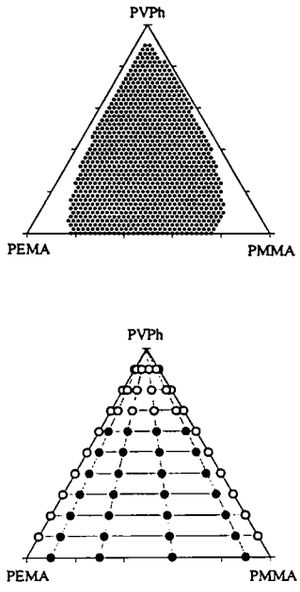

Figure 23 (Top) Theoretical ternary phase diagram for PEMA/PVPh/PMMA blends calculated at 25°C using the appropriate parameters listed in *Table 2*. (Bottom) Ternary phase diagram displaying the experimental data of Pomposo *et al.*[34]; the open circles represent compositions exhibiting a single T_g and the solid circles represent compositions exhibiting two T_gs

to produce a homogeneous ternary mixture. The PVAc/PVPh/STVPy[70] blend system, with the strongly compounding $\Delta\chi$ and ΔK effects, could be considered a rather extreme example, so we will now consider a seemingly more innocuous immiscible binary system, PMMA/PEMA, that one might suspect (wrongly, as it turns out) could be homogenized by PVPh.

PMMA/PVPh/PEMA ternary blends

Studies of the PMMA/PVPh/PEMA system has been reported by Pomposo and co-workers, who have independently extended the association model to ternary hydrogen-bonded systems[34]. Although the specific repeat units of PMMA and PEMA are chemically rather similar, differing only by a single methylene in the side group, the two polymers are not miscible*. The non-hydrogen-bonded solubility parameter values of PMMA and PEMA, calculated from group contributions, are quite close at 9.1 and 8.9 $cal^{1/2}\,cm^{-3/2}$, respectively, which implies a rather weak $\Delta\chi$ effect. Similarly, the ΔK effect is apparently relatively weak as the effective values of the inter-association equilibrium constants, K'_A [$=(37.5\times100)/84.9]=44.1$ and K'_C [$=(37.5\times100)/101.4]=37.0$, are quite similar. This is because the specific interactions between the phenolic hydroxyls and the two different methacrylate carbonyl groups are identical in this case, and the molar volumes of the specific repeats of PMMA and PEMA are not too dissimilar at 84.9 and 101.4 $cm^3\,mol^{-1}$, respectively. Thus, at first glance, one might anticipate a significant homogeneous area in the ternary phase diagram. Unfortunately, the contrary is true. The two effects ($\Delta\chi$ and ΔK) work in concert and the predicted ternary spinodal phase diagram (top of *Figure 23*) calculated from the parameters listed in *Table 2*, which is very similar to that calculated by Pomposo *et al.*[34], exhibits a large area of heterogeneity.

Conventional second run d.s.c. thermograms were performed by Pomposo *et al.*[34] and these data are reproduced on the ternary diagram at the bottom of *Figure 23* (open and solid circles again represent compositions that exhibited one or two T_gs, respectively). Ternary compositions rich in PVPh (>70%) were reported by Pomposo *et al.*[34] to exhibit single T_gs and this does not agree well with the predicted phase diagram. These authors correctly point out that the phase diagram is very sensitive to the values of the solubility parameters and suggest that the failure to completely match the observed data might be due to the errors inherent in the estimation of solubility parameters[1]. While this is certainly possible, one must also recognize the difficulty in experimentally establishing a single phase. As we have seen in this present work, a single T_g observed in a d.s.c. thermogram does not verify, *per se*, a single phase in ternary blends, especially in blends rich in one component. To illustrate this we repeated the conventional second run d.s.c. run on a sample of a PMMA/PVPh/PEMA blend having a composition of 10:80:10 and obtained a single T_g (*Figure 24A*), which agrees with the observation of Pomposo *et al.*[34]. After enthalpy relaxation studies were performed (*Figures 24B* and *C*), however, evidence of two compositions is observed, indicating the presence of more than one phase.

All in all, the theoretical predictions and the experimental observations for the PMMA/PVPh/PEMA blend system are in good agreement. And this is bad news for those wishing to homogenize even closely matched immiscible binary polymer blends (PolyA and PolyC) with a hydrogen bonding polymer (PolyB) that is miscible with both PolyA and PolyC. Only if we can counterbalance the competing forces ($\Delta\chi$ and ΔK) will it be possible to form truly homogeneous ternary blends over wide composition ranges, and these will be very special cases indeed. We end by indicating how one might attempt to find such a system by considering PMMA/PVPh/PTHF blends.

PMMA/PVPh/PTHF ternary blends — a theoretical prediction only

The predicted phase diagram for PMMA/PVPh/PTHF ternary blends at 25°C is shown in *Figure 25*. Two areas of heterogeneity are calculated: a closed loop skewed towards the PVPh-rich and PVPh/PMMA

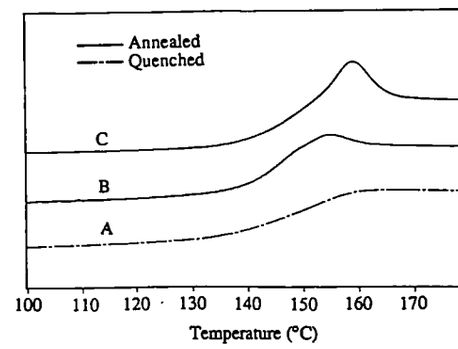

Figure 24 (A) Conventional second run d.s.c. thermogram for a blend composition containing 10:80:10 wt% PEMA/PVPh/PMMA and the corresponding thermograms obtained after physically ageing for (B) 3 h and (C) 15 h

* Using the range $(\delta\Delta)_{Crit}$ values from 0.1 (dispersive forces) to 0.5 (polar forces) $cal^{1/2}\,cm^{-3/2}$, ref. 1 predicts that blends of PMMA and PEMA should be 'on the edge' of miscibility

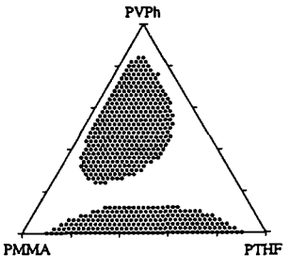

Figure 25 Theoretical ternary phase diagram for PMMA/PVPh/PTHF blends calculated at 25°C using the appropriate parameters listed in *Table 2*

binary axis, and a curved sector emanating from the PMMA/PTHF axis. The non-hydrogen-bonded solubility parameter of PTHF (8.8 $cal^{1/2}\,cm^{-3/2}$) is quite close to that of PEMA and like the PMMA/PVPh/PEMA system this implies a rather weak $\Delta\chi$ effect for PMMA/PVPh/PTHF blends. The ΔK effect, on the other hand is significant [$K'_A = (37.5 \times 100)/84.9 = 44.1$ and $K'_C = (88.0 \times 100)/71.1 = 124$] and in the opposite 'direction' to that of the PMMA/PVPh/PEMA system, which serves to counterbalance the $\Delta\chi$ effect for the PMMA/PVPh/PTHF blends. As a consequence, a significant portion of the ternary phase diagram is predicted to be homogeneous. Frankly, the values of the various parameters are not known with sufficient accuracy to expect the predicted phase diagram to approach reality, but it does suggest that experimental studies on PMMA/PVPh/PTHF and similar blends might be worthwhile.

ACKNOWLEDGEMENT

The authors gratefully acknowledge the financial support of the National Science Foundation, Polymers Program.

REFERENCES

1 Coleman, M. M., Graf, J. F. and Painter, P. C. 'Specific Interactions and the Miscibility of Polymer Blends', Technomic Publishing Inc., Lancaster, PA, 1991
2 Painter, P. C., Graf, J. F. and Coleman, M. M. *J. Chem. Phys.* 1990, **92**, 6166
3 Graf, J. F., Coleman, M. M. and Painter, P. C. *J. Phys. Chem.* 1991, **95**, 6710
4 Yang, X., Painter, P. C., Coleman, M. M., Pearce, E. M. and Kwei, T. K. *Macromolecules* 1992, **25**, 2156
5 Coleman, M. M., Yang, X., Painter, P. C. and Graf, J. F. *Macromolecules* 1992, **25**, 4414
6 Coleman, M. M., Yang, X., Zhang, H., Painter, P. C. and Scherer Jr, K. V. *J. Polym. Sci., Polym. Chem. Edn* 1993, **31**, 2039
7 Coleman, M. M., Yang, X., Zhang, H. and Painter, P. C. *J. Macromol. Sci. Phys.* 1993, **B32**, 295
8 Coleman, M. M., Yang, X., Painter, P. C. and Kim, Y. H. *J. Polym. Sci., Polym. Chem. Edn* 1994, **32**, 1817
9 Coleman, M. M., Yang, X., Stallman, J. B. and Painter, P. C. *Makromol. Chem.* submitted
10 Pomposo, J. A., Calahorra, E., Eguiazabal, I. and Cortazar, M. *Macromolecules* 1993, **26**, 2104
11 Pomposo, J. A., Cortázar, M. and Calahorra, E. *Macromolecules* 1994, **27**, 245
12 de Juana, R., Etxeberria, A., Cortázar, M. and Iruin, J. J. *Macromolecules* 1994, **27**, 1395
13 de Ilarduya, A. M., Eguiburu, J. L., Espi, E., Iruin, J. J. and Fernández-Berridi, M. J. *Makromol. Chem.* 1993, **194**, 501
14 Taylor-Smith, R. E. and Register, R. A. *Macromolecules* 1993, **26**, 2802
15 Scott, R. L. *J. Chem. Phys.* 1949, **17**, 279
16 Tompa, H. *Trans. Faraday Soc.* 1949, **45**, 1140
17 Flory, P. J. *J. Chem. Phys.* 1941, **9**, 660
18 Huggins, M. L. *J. Chem. Phys.* 1941, **9**, 440
19 Zeman, L. and Patterson, D. *Macromolecules* 1972, **5**, 513
20 Patterson, D. *Polym. Eng. Sci.* 1982, **22**, 64
21 Hsu, C. C. and Prausnitz, J. M. *Macromolecules* 1974, **7**, 320
22 Su, A. C. and Fried, J. R. *Polym. Eng. Sci.* 1987, **27**, 1657
23 ten Brinke, G., Karasz, F. E. and MacKnight, W. J. *Macromolecules* 1983, **16**, 1827
24 Paul, D. R. and Barlow, J. W. *Polymer* 1984, **25**, 487
25 Cowie, J. M. G., Li, G. X., Ferguson, R. and McEwen, I. J. *J. Polym. Sci., Polym. Phys. Edn* 1992, **30**, 1351
26 Shah, V. S., Keitz, J. D., Paul, D. R. and Barlow, J. W. *J. Appl. Polym. Sci.* 1986, **32**, 3863
27 Christiansen, W. H., Paul, D. R. and Barlow, J. W. *J. Appl. Polym. Sci.* 1987, **34**, 537
28 Rigby, D., Lin, J. L. and Roe, R. J. *Macromolecules* 1985, **18**, 2269
29 Landry, C. J. T., Yang, H. and Machell, J. S. *Polymer* 1991, **32**, 44
30 Koklas, S. N., Sotiropoulou, D. D., Kallitsis, J. K. and Kalfoglou, N. K. *Polymer* 1991, **32**, 66
31 Klotz, S. and Cantow, H.-J. *Polymer* 1990, **31**, 315
32 Le Menesterel, C., Bhagwagar, D. E., Painter, P. C. and Coleman, M. M. *Macromolecules* 1992, **25**, 7101
33 Coleman, M. M., Xu, Y., Painter, P. C. and Graf, J. E. 'ANTEC Conference Proceedings', Vol. 1, Society of Plastics Engineers, Brookfield, 1993, pp. 680–683
34 Pomposo, J. A., Cortázar, M. and Calahorra, E. *Macromolecules* 1994, **27**, 252
35 Min, K. E., Chiou, J. S., Barlow, J. W. and Paul, D. R. *Polymer* 1987, **28**, 172
36 Guo, Q. P. *Eur. Polym. J.* 1990, **26**, 1329; 1990, **26**, 1333
37 Brannock, G. R. and Paul, D. R. *Macromolecules* 1990, **23**, 5240
38 Eguiazabal, J. I., Iruin, J. J., Cortazar, M. and Guzman, G. M. *Cell. Chem. Tech.* 1985, **19**, 415
39 Perrin, P. and Prud'homme, R. E. *Acta Polym.* 1993, **44**, 307
40 Defew, G., Groeninckx, G. and Reynaers, H. in 'Contemporary Topics in Polymer Science, Vol. 6: Multiphase Macromolecular Systems' (Ed. B. M. Culbertson), Plenum Press, New York, 1989, pp. 423–438
41 Jo, W. H., Kwon, Y. K. and Kwon, I. H. *Macromolecules* 1991, **24**, 4708
42 Kwei, T. K., Fisch, H. L., Radigan, W. and Vogel, S. *Macromolecules* 1977, **10**, 157
43 Wang, Y. Y. and Chen, S. A. *Polym. Eng. Sci.* 1981, **21**, 47
44 Eguiazabal, J. I., Iruin, J. J., Cortazar, M. and Guzman, G. M. *J. Appl. Polym. Sci.* 1986, **32**, 5945
45 Goh, S. H. and Siow, K. S. *Thermochim. Acta* 1986, **102**, 281; 1986, **105**, 191
46 Huang, J. C., Min, K. and White, J. L. *Polym. Eng. Sci.* 1988, **28**, 1085
47 Ameduri, B. and Prud'homme, R. E. *Polymer* 1988, **29**, 1052
48 Iruin, J. J., Eguiazabal, J. I. and Guzman, G. M. *Eur. Polym. J.* 1989, **25**, 1169
49 Remiro, P. M. and Nazábal, J. *J. Appl. Polym. Sci.* 1991, **42**, 1475
50 Karcha, R. J. and Porter, R. S. *Polymer* 1992, **33**, 4866
51 Kim, W. N., Park, C. E. and Burns, C. M. *J. Appl. Polym. Sci.* 1993, **49**, 1003
52 Struik, L. C. E. 'Physical Aging in Amorphous Polymers and Other Materials', Elsevier, Amsterdam, 1978
53 Kovacs, A. J., Aklonis, J. J., Hutchinson, J. M. and Ramos, A. R. *J. Polym. Sci., Polym. Phys. Edn* 1979, **17**, 1097
54 Hodge, I. M. *Macromolecules* 1987, **20**, 2897
55 Cowie, J. M. G. and Ferguson, R. *Macromolecules* 1989, **22**, 2312
56 Oudhuis, A. A. C. M. and ten Brinke, G. *Macromolecules* 1992, **25**, 698
57 Bosma, M., ten Brinke, G. and Ellis, T. S. *Macromolecules* 1988, **21**, 1465
58 Grooten, G. and ten Brinke, G. *Macromolecules* 1989, **22**, 1761
59 ten Brinke, G. and Grooten, R. *Colloid Polym. Sci.* 1989, **267**, 992
60 Ellis, T. S. *Macromolecules* 1990, **23**, 1494
61 Coleman, M. M., Xu, Y., Painter, P. C. and Harrell, J. R. *Makromol. Chem., Macromol. Symp.* 1991, **52**, 75
62 Coleman, M. M., Zhang, H., Xu, Y. and Painter, P. C. *Am. Chem. Soc. Adv. Chem. Ser.* 1993, **236**, 221
63 Painter, P. C., Veytsman, B. and Coleman, M. M. *J. Polym. Sci., Polym. Chem. Edn* 1994, **32**, 1189
64 Coleman, M. M., Xu, Y. and Painter, P. C. *Macromolecules* 1994, **27**, 127
65 Veytsman, B. and Painter, P. C. *J. Chem. Phys.* in press
66 Moskala, E. J., Howse, S. E., Painter, P. C. and Coleman, M. M. *Macromolecules* 1984, **17**, 1671
67 Coleman, M. M., Lichkus, A. M. and Painter, P. C. *Macromolecules* 1989, **22**, 586

68 Nandi, A. K., Mandal, B. M., Bhattacharya, S. N. and Roy, S. K. *Polym. Commun.* 1986, **27**, 151
69 Fernandes, A. C., Barlow, J. W. and Paul, D. R. *J. Appl. Polym. Sci.* 1986, **32**, 6073
70 Fox, T. G. *Bull. Am. Phys. Soc.* 1956, **1**, 123
71 Bhagwagar, D. E., Painter, P. C. and Coleman, M. M. *Macromolecules* 1992, **25**, 1361
72 Moskala, E. J., Varnell, D. F. and Coleman, M. M. *Polymer* 1985, **26**, 228
73 Serman, C. J., Xu, Y., Painter, P. C. and Coleman, M. M. *Polymer* 1991, **32**, 516
74 Quin, C., Pires, A. T. N. and Belfoire, L. A. *Polym. Commun.* 1990, **31**, 177
75 Munoz, E., Calahorra, E., Cortázar, M. and Santamaria, A. *Polym. Bull.* 1982, **7**, 295
76 Martuscelli, E., Silvestre, C. and Gismondi, C. *Makromol. Chem.* 1985, **186**, 2161
77 Silvestre, C., Karasz, F. E., MacKnight, W. J. and Martuscelli, E. *Eur. Polym. J.* 1987, **23**, 745
78 Han, C. D., Chung, H. S. and Kim, J. K. *Polymer* 1992, **33**, 546
79 Powell, D. L. and West, R. *Spectrochim. Acta* 1964, **20**, 983
80 Meftahi, M. V. and Frechet, J. M. J. *Polymer* 1988, **29**, 477